Spring 2012

Analysis of chronic obstructive pulmonary disease (COPD) using CT images

Sandeep Bodduluri
University of Iowa

Recommended Citation

Bodduluri, Sandeep. "Analysis of chronic obstructive pulmonary disease (COPD) using CT images." MS (Master of Science) thesis, University of Iowa, 2012.
https://doi.org/10.17077/etd.f7k0hz6i

ANALYSIS OF CHRONIC OBSTRUCTIVE PULMONARY DISEASE (COPD)

USING CT IMAGES

by

Sandeep Bodduluri

A thesis submitted in partial fulfillment
of the requirements for the Master of
Science degree in Biomedical Engineering
in the Graduate College of
The University of Iowa

May 2012

Thesis Supervisor: Professor Joseph M. Reinhardt

Graduate College
The University of Iowa
Iowa City, Iowa

CERTIFICATE OF APPROVAL

_____

MASTER'S THESIS

_____

This is to certify that the Master's thesis of

Sandeep Bodduluri

has been approved by the Examining Committee for the
thesis requirement for the Master of Science degree in
Biomedical Engineering at the May 2012 graduation.

Thesis Committee: _____
                    Joseph M. Reinhardt, Thesis Supervisor

                  _____
                    John D. Newell

                  _____
                    Jessica C. Sieren

                  _____
                    Gary E. Christensen

                  _____
                    Mona K. Garvin

To my family and friends.

Failure is simply the opportunity to begin again,
this time more intelligently.

Henry Ford

ACKNOWLEDGMENTS

ABSTRACT

Chronic Obstructive Pulmonary Disease (COPD), a growing health concern, is the fourth leading cause of death in the United States. While people habituated to smoking constitute the highest COPD susceptible population, people exposed to air pollution or other lung irritants also form a major group of potential COPD patients. COPD is a progressive disease that is characterized by the combination of chronic bronchitis, small airway obstruction, and emphysema that causes an overall decrease in the lung elasticity affecting the lung tissue. The current gold standard method to diagnose COPD is by pulmonary function tests (PFT) which measures the extent of COPD based on the lung volumes and is further classified into five severity stages. PFT measurements are insensitive to early stages of COPD and also its lack of reproducibility makes it hard to rely on, in assessing the disease progression. Alternatively, Pulmonary CT scans are considered as a major diagnostic tool in analyzing the COPD and CT measures are also closely related to the pathological extent of the disease. Quantification of COPD using features derived from CT images has been proven effective. The most common features are density based and texture based. We propose a new set of features called lung biomechanical features which capture the regional lung tissue deformation patterns during the respiratory cycle. We have tested these features on 75 COPD subjects and 15 normal subjects. We have done classification of COPD/Non COPD on the dataset using the three feature sets and also performed the classification all these subjects to their corresponding severity stage. It is shown that the lung biomechanical features were also able to classify COPD subjects with a good AUC. It is also shown that, by combining the best features from each feature set, there is an improvement in the classifier performance. Multiple regression analysis is performed to find the correlation between the CT derived features and PFT measurements.

TABLE OF CONTENTS

LIST OF TABLES

LIST OF FIGURES

CHAPTER 1

INTRODUCTION

1.1. Motivation

Chronic Obstructive Pulmonary Disease (COPD), a growing health concern, is the fourth leading cause of death in the United States[1, 2]. While people habituated to smoking constitute the highest COPD susceptible population, people exposed to air pollution or other lung irritants also form a major group of potential COPD patients. COPD is a progressive disease that is characterized by the combination of chronic bronchitis, small airway obstruction, and emphysema that causes an overall decrease in the lung elasticity affecting the lung tissue. The current gold standard method to diagnose COPD is by pulmonary function tests (PFT) which measures the extent of COPD based on the lung volumes. The insensitivity of PFT to the early stages of the disease, its evaluation based on global lung function and also its lack of reproducibility makes it hard to rely on, in assessing the disease progression [3, 4]. These tests are also labor intensive and time consuming. Alternatively, Pulmonary CT scans are considered as a major diagnostic tool in analyzing COPD and CT measures are also closely related to the pathological extent of the disease [5, 6]. CT imaging of the lungs provides important information about airflow patterns in the COPD subjects. Densitometry analysis of CT images has been successfully used to distinguish COPD subjects from normal[7-11]. Recently, textural patterns on the CT images showed significant difference in the disease progression and are proved useful in detecting COPD subjects[12-16]. Quantification of COPD based on the features derived from CT images has been recognized effective and these features are correlated well with PFT measurements[13-15]. There are several other features of CT that are closely related to the lung function[17-20]. By the use of machine learning, the capability of various features in diagnosing and staging COPD can be evaluated and the best

combination of features can be extracted. These features may result in better diagnosis of COPD and the evaluation of its progression at different stages.

1.2. The State of the Art

Several methods are proposed to diagnose COPD using CT images. Gould et al. proposed a lowest fifth percentile method based on CT attenuation values to calculate the pathological extent of emphysema[17-22]. Later, Muller et al. proposed 'Density Mask' method based on the relative area of low attenuation values in CT to detect emphysema. This method calculates the percentage of voxels below a certain threshold which gives the extent of emphysema. A threshold range of -910HU to -960HU was shown capable of providing the emphysema extent [8]. Genevois et al. compared density measurements with the pathological extent of emphysema and found significant correlations with the extent of emphysema at a threshold of -950HU[7]. Shaker et al. and other groups used these density based measurements and showed lowest 15th percentile of the frequency distribution provided the estimate of emphysema in $alpha_1$ antitrypsin-deficient individuals[23, 24] . In addition to the emphysema scores from CT, Newman et al. calculated the extent of air trapping in asthma patients using expiratory CT images. This method calculates the percentage of low attenuation values in expiratory CT below a threshold of -900HU [11]. Matsuoka et al. calculated the air trapping measure in COPD subjects and found the decreased attenuation values below -860HU in the expiratory CT is significantly correlated with the airway dysfunction regardless of emphysema[25]. The ratio of mean lung density on expiration and inspiration is also used to estimate air trapping. Lee et al. evaluated the correlation between the emphysema, air trapping scores of COPD subjects with the clinical parameters. They have shown that the CT parameters are well correlated with the PFT, body mass index scores [26]. Murphy et al. performed the classification at each severity stage of COPD using 3D registration of inspiration and

expiration images. Registration based features are shown working better than the normal density based features of CT [27]. Lederman et al. compared the density based metrics with the lung function and showed the higher density lung regions also provide clinical information regarding the COPD severity [28]. Although the density based measurements are proved to be effective in detecting emphysema and airway obstruction, textural patterns on CT images of COPD patients are also found to be valuable. Uppaluri et al. proposed the adaptive multiple feature method (AMFM) to classify emphysema using textural patterns on pulmonary CT images. First order and second order statistical features of texture patterns were used to classify emphysematous lung tissue [15]. This method showed good accuracy in classifying emphysema subjects and normal subjects. Sorensen et al. also used textural features in classifying moderate to severe COPD subjects from normal subjects. Disease probability given to the image by fusing individual probabilities evaluated at local region of interests (ROI) in the images. The ROI classification is based on k nearest neighbor classifier with features from a multi scale Gaussian filter bank. All the ROI probabilities are combined to give a single probability for the image using a posterior probability estimate[13, 14]. Various authors used the texture and density based approach to diagnose various lung pathologies and have shown these approaches are compared well with the structural changes happening in the lungs as the disease progresses [12, 29, 30]. The most common textural features are gray level co-occurrence matrices (GLCM), run length matrices (RLM), Gaussian filter bank features. Recently, Murphy et al. used regional ventilation measures from the registration of inspiration and expiration images as a new feature set to classify COPD subjects to their corresponding severity stage [18]. Also, features based on tracheal changes in the CT images are used to classify COPD subjects [20]. Most of these features classified COPD subjects with good accuracy and correlated well with PFT measurements.

1.3. New Approaches

We performed the classification of COPD using a new set of lung biomechanical features derived by the registration of inspiratory and expiratory CT in addition to the current texture based and density based features. The new set of features is calculated based on the estimates of regional lung tissue expansion and contraction and are compared well with the function of lungs[17, 19, 31]. These features capture the mechanical changes that occur in the lung from inspiration to expiration. As a part of five classification experiments, we have tested the effectiveness of these features in distinguishing normal subjects from the severely diseased in comparison with the texture and density based features. We have also performed classification of normal versus COPD subjects at all the stages (mild to very severe) using density, texture and lung biomechanical features. As the final step of classification, we have classified COPD subjects in to their corresponding severity stage. For all these experiments, we have added an extra feature set which is the combination of best features from density, texture and lung biomechanical feature sets. We have done this analysis at whole lung level and lobar level. We compared our results to the PFT measurements.

In the following chapters of this thesis, we give background information about COPD and quantitative analysis of COPD using pulmonary CT in chapter 2. We described our dataset, preprocessing techniques and the methodology of calculating the features in chapter 3. Also in chapter 3, we described the feature selection, classification and implementation details. In chapter 4, we showed our classification results in at whole lung level and lobar level. In chapter 5, we discussed the significance of this research and the future work.

CHAPTER 2

BACKGROUND

2.1. CHRONIC OBSTRUCTIVE PULMONARY DISEASE (COPD)

<u>2.1.1. Definition and Overview</u>

COPD is an airflow obstruction disease which is caused by emphysema and/or chronic bronchitis. It narrows the airways, leading to the progressive reduction of the airflow in and out of the lungs. COPD is considered as a major public health problem, as it is the fourth leading cause of death in United States [1, 2]. Smoking is the major risk factor that causes COPD. According to Global Initiative for the Chronic Obstructive Lung Disease (GOLD) guidelines, a general definition of COPD is

Chronic obstructive pulmonary disease (COPD) is a preventable and treatable disease with some significant extra pulmonary effects that may contribute to the severity in individual patients. Its pulmonary component is characterized by airflow limitation that is not fully reversible. The airflow limitation is usually progressive and associated with an abnormal inflammatory response of the lung to noxious particles or gases.[1, 2]

The interrelationship between emphysema and bronchitis makes it harder to find a single factor that is contributing towards the disease progression. Emphysema causes the destruction of the lung tissue that is necessary to support the physical shape and function of the lungs. It destroys the lung tissue which leads to dyspnea. Emphysema is classified into three subtypes; centrilobular, panlobular, and paraseptal emphysema. In centrilobular, the respiratory bronchiole is affected and occurs more commonly in the upper lobes. Panlobular emphysema causes the expansion of entire respiratory acinus and occurs in lower lobes. Paraseptal occurs at lung peripheral structures. Chronic bronchitis is the inflammation of airways. It causes cough with sputum production. There will be an increased mucus accumulation in the airways which leads to the narrowing of the airways and causing a cough. According to the Global Initiative for the Chronic Obstructive Lung

Disease (GOLD) guidelines, the prevalence of COPD is now almost equal in men and women and is directly related to smoking. Tobacco smoking is the important risk factor of COPD. The major percentage of COPD patients are smokers or have smoked. Smoking causes the alterations of surfactant quality and also hyperplasia, hypertrophy of mucus secreting glands. The people who have a prolonged exposure to the outdoor environment like dust, fumes, and polluted gas surroundings are more susceptible to COPD than the general population[1]. In these cases, air flow obstruction is caused by hyper secretion of mucus with the pollutants reaching terminal bronchi and alveoli. Also, the deficiency of alpha$_1$ antitrypsin is a significant genetic factor that causes COPD[11, 24]. All these risk factors illustrate that the development of the disease is also related to genetic factors and environmental exposures. It is also shown that a COPD subject may undergo cardiac failure due to airflow obstruction and hyperinflation caused by COPD. Some of the comorbidities associated with COPD are heart diseases, diabetes, osteoporosis, and skeletal muscle dysfunction and lung cancer[1].

2.1.2. Diagnosis

Evaluation for COPD is recommended for any patient who has dyspnea, chronic cough and/or exposed to any of the risk factors for the disease. Dyspnea is a cardinal symptom of the disease which increases the effort to breathe or causes gasping and it worsens over the disease progression. Chronic cough and sputum production is also an important symptom while diagnosing and it is intermittent at the early stages but worsens at the severe stage of COPD.
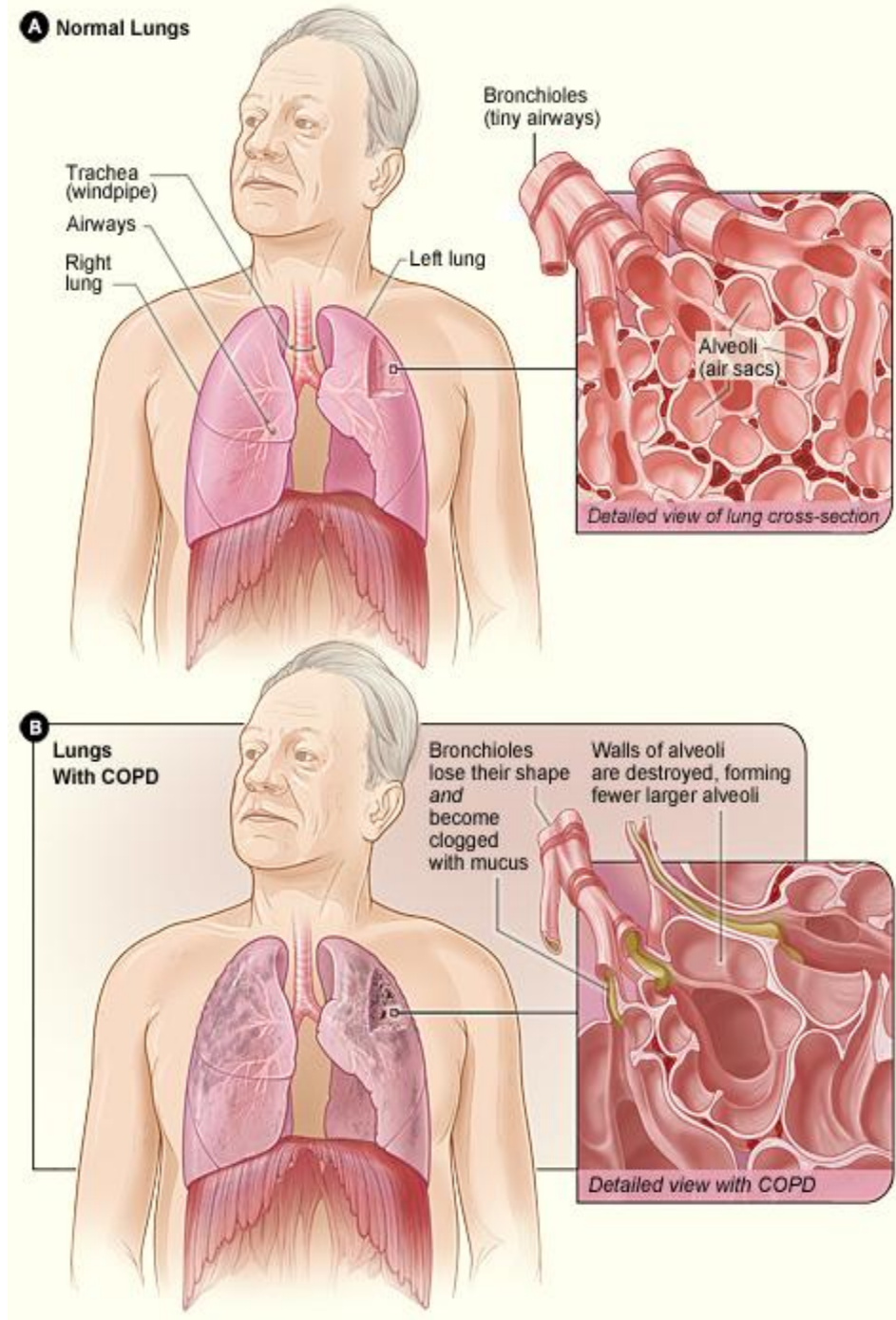
Figure 1: Emphysema and Chronic Bronchitis in COPD, Adapted from [32].

Additional symptoms are fatigue, weight loss which can be the signs of other diseases associated with the COPD. Depression and anxiety are also common at the severe stages of COPD. COPD assessment is done by performing spirometry or Pulmonary Function Test (PFT) which is a current gold standard diagnosis of COPD. PFT measures the lung volumes at different stages of breathing by asking the subject to breathe into a mouthpiece connected to a spirometer. COPD is diagnosed based on two lung volumes; the maximum volume of air that can be forcibly blown out after full inspiration, called as forced vital capacity (FVC), and the maximum volume of air that one can blow out in the first second of the FVC process called as forced expiratory volume at the first second of the expiration (FEV_1). If FEV_1/FVC is less than 0.7, then the subject is considered as a potential COPD subject suffering from airflow obstruction. Normalization of FEV_1 according to expected value based on age, height, sex is called $FEV_1\%$ predicted of that specific patient. This measure is used to estimate the severity of the disease.

According to the Global Initiative for the Chronic Obstructive Lung Disease (GOLD) guidelines, COPD is classified in to five severity stages as explained in Table 1. GOLD0 is an asymptotic stage of the disease where subjects are likely to get COPD. GOLD1 is a mild stage where airflow limitation is mild and usually the patient is unaware that the lung function is not normal. GOLD2 is a moderate stage of COPD at which patients usually feel shortness of breath and typically seek medical attention. GOLD3 is a severe stage of the disease where the patient experiences greater shortness of breath, fatigue and reduced exercise capacity. GOLD4 is a very severe stage of COPD characterized by severe air flow limitation and the chronic respiratory failure. Patient's quality of life is severely worsens at this stage.

COPD CLASS	PFT Measurement
GOLD0 (Asymptotic)	$FEV_1/FVC > 0.7$
GOLD1 (Mild)	$FEV_1/FVC < 0.7$; $FEV_1\%pred > 80\%$
GOLD2 (Moderate)	$FEV_1/FVC < 0.7$; $50\% < FEV_1\%pred < 80\%$
GOLD3 (Severe)	$FEV_1/FVC < 0.7$; $30\% < FEV_1\%pred < 50\%$
GOLD4 (Very Severe)	$FEV_1/FVC < 0.7$; $FEV_1\%pred < 30\%$

Table 1**:** COPD severity stages according to GOLD guidelines.

There are other validated questionnaires to estimate the impact of the disease on the daily life activities of a patient. Modified British Medical Research Council (mMRC) or COPD Assessment Test (CAT) is the common measure. It is used to assess the health impairment caused by COPD on patient's daily life activities. It is an 8-item health status questionnaire which has the score ranging from 0-40. St. George's Respiratory Questionnaire (SGRQ) is another important questionnaire which is designed to measure health impairment in patients with asthma and COPD. The first section of SGRQ evaluates symptoms like frequency of cough, sputum production and breathlessness. The second section is of two components: activity and impact scores. Activity section evaluates the activities that cause breathlessness and the impacts section covers the impact of the diseases on several day to day activities. SGRQ score has been shown to correlate well with established measures of symptom level, disease activity and disability. 6-minute walk test (6MWT) is also a useful measure of functional capacity, which evaluates the exercise capacity of moderate to high severity stages of the disease. The American Thoracic Society provided guidelines to perform the test and to measure the response for pulmonary and cardiac diseases. Modified medical research council's (MMRC) dyspnea scale including body mass index, airflow obstruction and exercise

capacity from 6MWT can be used to estimate the bode index [1, 2]. Bode index is used to calculate the life expectancy of a COPD patient. All these measures are used to diagnose COPD and to evaluate its progression at each severity stage.

2.2. Quantification of COPD Using Pulmonary CT

Pulmonary function test measurements do not provide regional assessment of the disease in the lung. It is solely based on global lung volume measurements. In contrast, computed tomography (CT) allows regional assessment of lung function and has been shown pathologically related to chronic bronchitis and emphysema components of COPD[5, 6]. The quantification of emphysema in CT is based on low attenuation areas in CT images of the lung, i.e. regions of parenchymal destruction. Gould et al. measured the emphysema extent using CT attenuation values and fifth percentile values of CT attenuation histogram. In 1988, Muller et al. used a commercially available GE CT software 'Density Mask' and found high correlations of emphysema with attenuation values lower than -910HU. Later, Genevois et al. applied various thresholds ranging from -910HU to -970HU to measure emphysema extent. They showed that the attenuation values lower than threshold -950HU on high resolution CT images obtained at full inspiration as the best emphysema measure. Expiratory CT is shown to be useful for airway obstruction and air trapping measures more than it does emphysema [9, 11]. Recently, Murphy et al used the percentage of voxels below -850HU from the expiratory CT and found high correlations with pulmonary function measurements [18].

Texture analysis of CT images is another approach for the quantification of COPD[13-16, 33, 34]. Uppaluri et al. developed adaptive multiple feature method (AMFM) based on textural patterns of CT images obtained at full inspiration [15]. They have used two dimensional sections of the whole lung to capture grey level differences on the images. First order statistical features: mean, median, skewness, kurtosis and variance

were computed for each region in the lung. Also, the second order statistics: entropy, contrast and angular second moment were computed. They have shown that these textural features were sensitive to spatial relationships between pixels in a region allowing them to discriminate emphysema regions from normal regions in the lung. They compared AMFM with mean lung density and fifth percentile methods. AMFM achieved 100% accuracy in classifying normal from emphysema regions. However, AMFM method has no significant correlations with the pulmonary function test measurements[15, 35]. The two dimensional AMFM is later extended to a three dimensional texture based approach to differentiate normal lung from subtle lung pathologies by Xu et al.[16, 34]. They have computed 24 features for each region and used Bayesian classifier for discrimination. They have shown that the 3D AMFM was able to find the textural differences on the normal appearing lung from the population of nonsmokers and normal smokers. 3D AMFM is shown to be more sensitive and specific than the earlier 2D AMFM in discriminating smoking related lung pathologies. Gaussian filtering of CT images at multiple scales is another approach followed by Sorensen et al. to quantify COPD[13]. An automatic data driven approach for texture based quantitative analysis was proposed. Rotation invariant local binary patterns and a rotation invariant filter bank of Gaussian derivatives were computed for local regions of interests (ROI) in the lungs. A quantitative measure of COPD is obtained by fusing ROI probabilities, computed using a k nearest neighbor (kNN) classifier. The proposed measure achieved an AUC of 0.713 in classifying subjects with and without COPD, whereas the best density based emphysema measure achieved an AUC of 0.596. They have also shown better correlations with lung function and the robustness to inspiration level changes.

Although density based and texture based features were successful in quantification of COPD, these features were calculated from the inspiration and expiration scan alone. Murphy et al. used features from the transformed image obtained by the registration of inspiratory and expiratory CT to classify COPD subjects[27].

Average ventilation is computed through the comparison of HU value changes between inspiratory and expiratory CT scans using automatic non rigid registration. They have performed a classification of 110 COPD subjects with a 2-class KNN classifier (COPD/Non-COPD) and a 5-class classifier (COPD 1-4/Non-COPD). The registration based features achieved an AUC of 0.92 in the two class classification and 66% accuracy in the five class classification. Recently, the same group computed eleven different ventilation measurements based on the registration of inspiratory and expiratory CT [18]. These ventilation measurements were calculated from whole lung and lobar regions. They have achieved a 67% accuracy using registration based features in classifying 216 subject dataset to their corresponding GOLD severity. These registration based ventilation measurements demonstrated better correlations with pulmonary function test measures[18].

In this study, we proposed a new feature set called lung biomechanical feature set, consisting of regional lung tissue expansion and contraction estimates. These features are computed from displacement field information provided by the registration of inspiratory and expiratory CT scans. These features capture the mechanical changes during the lung function[17, 19, 31]. We have performed five classification experiments to test the effectiveness of these features in recognizing COPD and its level of severity. We have compared our results with the existing density based and texture based features. We combined our proposed features with the density and textural features to form a new feature set and evaluated its performance in COPD classification experiments.

CHAPTER 3

MATERIALS AND METHODS

3.1. Dataset

All the subjects in this study are selected from the Iowa cohort of the nationwide COPDGene database. All the data were gathered under a protocol approved by our Institutional Review Board. All the images were acquired with the subjects in the head first supine orientation on a Siemens sensation 64 multi-detector (MDCT) scanner (Siemens Medical Solutions, Enlargen, Germany). The scans followed an imaging protocol with the x-ray tube current 200 mAs, a tube voltage 120 kV, slice thickness of 0.75 mm, and a field of view of 500 mm. All the CT scans were acquired during breath-holds near function residual capacity (FRC)/full expiration and total lung capacity (TLC)/full inspiration in the same scanning session. Each scan was acquired at a reconstruction matrix of 512 by 512 with pixel spacing of (1 mm, 1 mm) and kernel B30f.
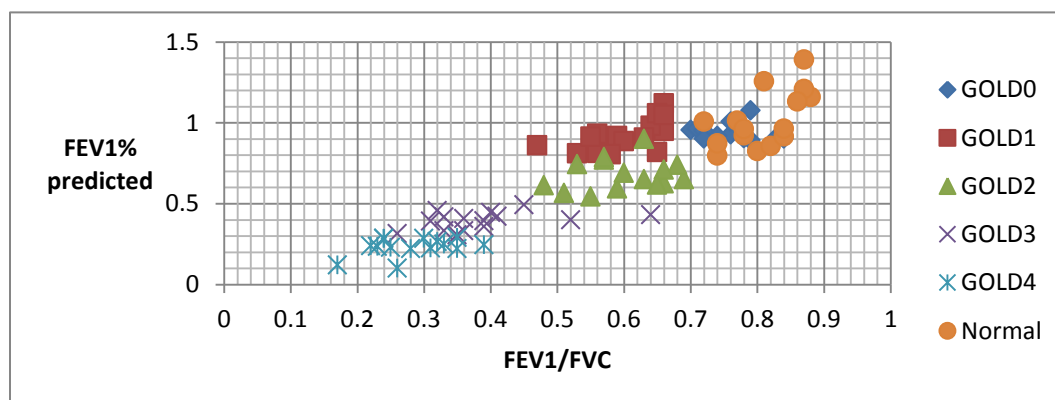
Figure 2: Graph showing the COPD subject information according to GOLD severity and PFT measurements.

We have selected a total of 90 subjects to use in this study with 15 subjects per each severity stage including 15 nonsmoking control subjects with normal PFT. The severity range of subjects used in this study according to the PFT measurements is shown in figure 2. The demographic information and pulmonary function measures of the data are shown in table 2. The complete demographic information per subject is listed in appendix.

Parameters	Non-COPD	COPD
Age	67.4 (6.79)	67.6 (5.87)
Gender (M/F)	15/15	31/29
Height (cm)	168.5 (8.66)	168.2 (9.02)
Weight (kg)	81 (11.8)	79.9 (21.3)
BMI	28.5 (4.08)	28.01 (6.26)
Pack years	-	39.05 (12.21)
FEV_1% predicted	0.9 (0.13)	0.55 (0.27)
FEV_1/FVC	0.7 (0.05)	0.46 (0.15)
GOLD STAGE (N/0/1/2/3/4)	15/15/0/0/0/0	0/0/15/15/15/15

All the numbers are mean values with standard deviation in parenthesis except GOLD stage and Gender

Table 2: Demographic information and PFT measures of the dataset used.

3.2. Overview of Methodology – Flowchart
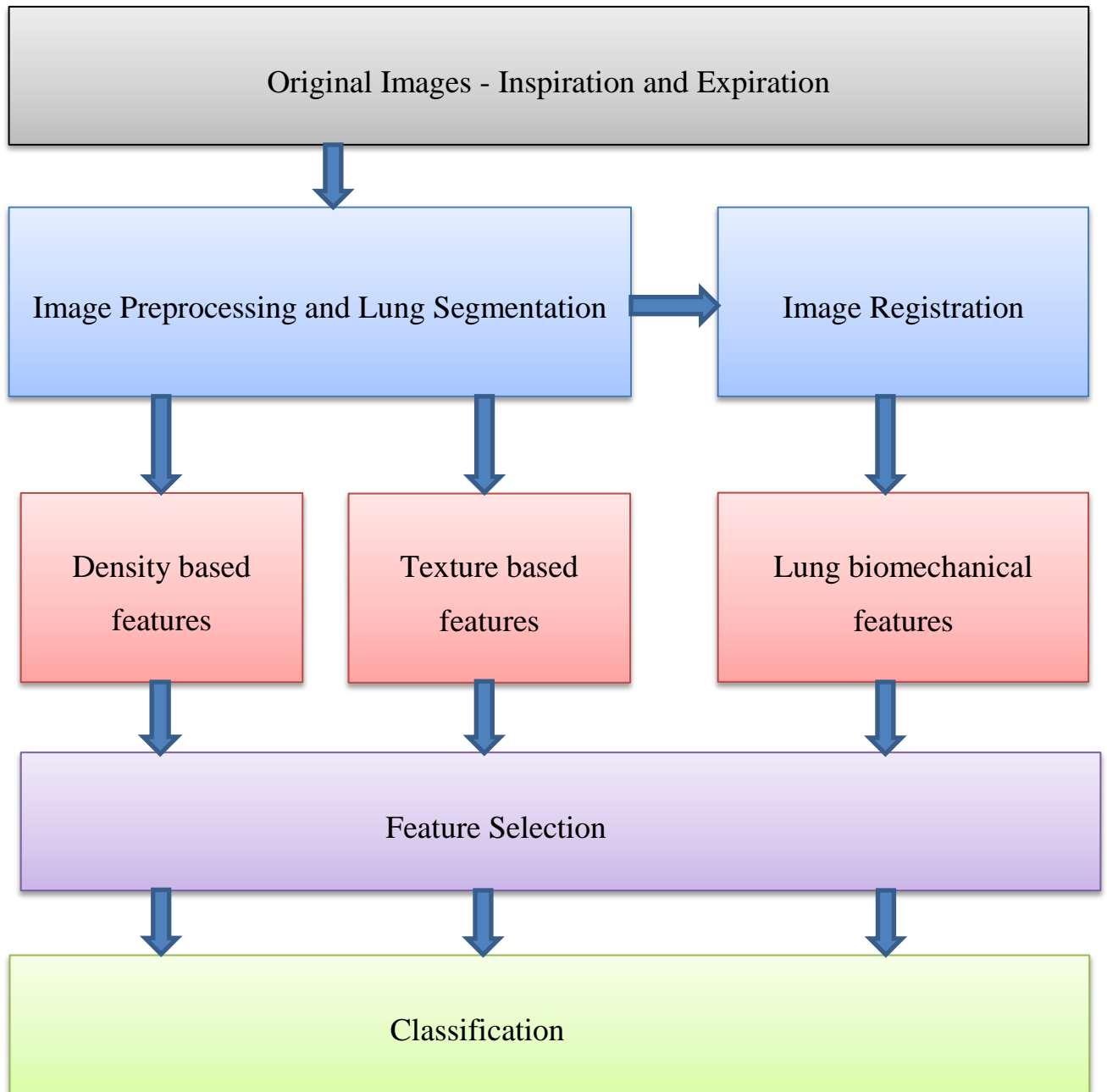
Figure 3: Workflow

The flowchart in figure 3, explains the workflow implemented in this study. The detailed description of each step is given in following sections of the chapter.

3.3. Image Preprocessing and Lung Segmentation

All volumetric CT data were converted from DICOM format and stored in 16-bit Analyze (Mayo Clinic, Rochester, MN) format [36]. Processing of CT data requires memory intensive tasks. Resampling of the data is done to maintain consistent spacing and resolution in all the images. To produce binary lung masks, region growing segmentation is carried out to segment the lungs. Region growing segmentation is a region based segmentation procedure that segments the given image into regions based on the discontinuities in the gray level and by the selection of initial seed points in the region. The segmentation is carried out on Analyze image processing software.

3.4. Image Registration

3.4.1. Basics of Image Registration

In order to do the mechanical analysis of lung, we have to capture the deformation changes happening from inspiration to the expiration image. This can be done by mapping of one image to the other in a single coordinate system. Image registration, a spatial transform mapping of one image into another as shown in the figure 4, is the solution for this problem. Many image registration algorithms have been proposed and various features were used to define the correspondences between two images[37, 38]. The basic components of the registration framework: two input images, a transform, a cost function, an interpolator, and an optimizer. The two inputs to the registration process are the moving or template image and fixed or target image. The transform used in the registration defines the deformational changes between the two images. The interpolator

is used to evaluate intensities in the moving image. The cost function contains a similarity metric measuring how well the fixed target image is matched by the transformed moving template image. Optimizer in the registration process optimizes the quantitative criterion formed by the similarity metric over the search space defined by the parameters of the transform. Registration is mainly dependent on the cost function. The spatial locations of corresponding voxels in a sequence of pulmonary scans are determined through the registration.
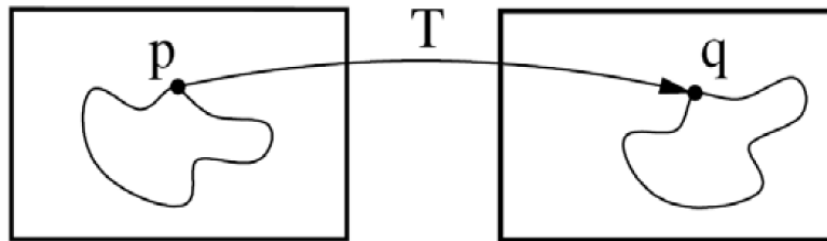
Figure 4 : Image registration is the task of spatial transformation mapping on one image to another. This figure is the schematic representation of this concept with a point p in the left image is mapped to a point q in the right image using transformation T. Adapted from[39]
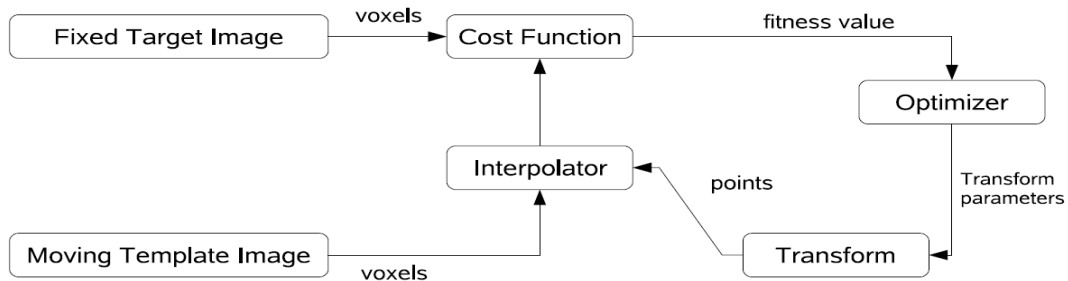
Figure 5: The basic components of the registration framework are two input images, a transform, a cost function, an interpolator, and an optimizer. Adapted from [39]

3.4.2. Registration Process

The inspiratory and expiratory CT images are registered for each subject since this pair of images shows large volume change and tissue deformation patterns of the lungs. We have used a lung mass preserving registration method to capture these differences between the images. This method uses a similarity metric called the sum of squared tissue volume difference (SSTVD), which estimates the local tissue and air fraction by minimizing local tissue mass difference [40, 41]. This method has been shown effective in lung image registration protocols[19, 42]. The tissue volume V in a voxel at position $\mathbf{X}$ can be estimated as

$$V(\mathbf{X}) = v(\mathbf{X}) \frac{HU(\mathbf{X}) - HU_{air}}{HU_{tissue} - HU_{air}} = v(\mathbf{X}) \, \beta\big(I(\mathbf{X})\big) \tag{3.1}$$

where $v(\mathbf{X})$ is the volume of voxel x [45]. Similarly, the air volume V' in a voxel can be estimated as

$$V'(\mathbf{X}) = v(\mathbf{X}) \frac{HU_{tissue} - HU(\mathbf{X})}{HU_{tissue} - HU_{air}} = v(\mathbf{X}) \propto \big(I(\mathbf{X})\big) \tag{3.2}$$

Where the sum of $\propto \big(I(\mathbf{X})\big)$ and $\beta\big(I(\mathbf{X})\big)$ is equal to 1 and $HU_{tissue} = 0HU$ and $HU_{air} = $ -1000HU. Then

$$\propto (\mathbf{X}) = \frac{-HU(\mathbf{X})}{1000}, \qquad \beta(X) = \frac{HU(\mathbf{X}) + 1000}{1000} \tag{3.3}$$

Let $I_1(\mathbf{X})$ and $I_2(\mathbf{X})$ be the intensity values, $v_1(\mathbf{X})$ and $v_2(\mathbf{X})$ be the voxel volumes, and $V_1(\mathbf{X})$ and $V_2(\mathbf{X})$ be the tissue volume in the voxel of images I_1 and I_2 respectively. Then the SSTVD is defined as [19, 42]

$$
\begin{aligned}
C_{SSTVD} &= \int_\Omega \left[V_2(\mathbf{X}) - V_1(h(\mathbf{X}))\right]^2 dx \\
&= \int_\Omega \left[V_2(\mathbf{X})\beta(I_2(\mathbf{X})) - V_1\left(h(\mathbf{X})\beta\left(I_1(h(\mathbf{X}))\right)\right)\right]^2 dx
\end{aligned} \tag{3.4}
$$

The Jacobian of a transformation J (h) estimates the local volume changes resulted from mapping an image through the deformation. Thus, the tissue volumes in image I_1 and I_2 are related by

$$
v_1(h(\mathbf{X})) = v_2(\mathbf{X}).J(h(\mathbf{X})). \tag{3.5}
$$

The registration process provides the displacement field information corresponding to the tissue deformation patterns in the lung from inspiration to expiration.

3.5. Feature Calculation

In this study, we have calculated three sets of features from the CT images. The three sets are: density based feature set which explains emphysema and air trapping extent, textural feature set which captures textural patterns based on multi scale derivatives of Gaussian filter bank, and the lung biomechanical feature set which captures the mechanical changes happening in the lung from the registration process. Density based feature set has only two features which are the direct estimates of emphysema and air trapping. In the texture based feature set, three filters were calculated at three different standard deviation values giving 9 filtered versions for each expiration image in the dataset. We have calculated five first order statistical features: mean, median, skewness,

kurtosis and standard deviation for each of these 9 filtered versions. Therefore, a total of 45 features formed a texture based feature set. Similarly, in the lung biomechanical feature set, 15 features were computed based on five statistical measures of three feature images. The summary of 62 features from the three feature sets is shown in table 3 and the feature calculation is described in the subsequent sections.

Feature Set	Feature Image	Features Calculated	Number of Features
Density based	1. Inspiration 2. Expiration	Emphysema Percentage of voxels below -950HU Air Trapping Percentage of voxels below -856HU	2
Textural (filtering at three different scales/standard deviations)	1. Base gaussian 2. Gradient magnitude of gaussian 3. Laplacian of the gaussian	mean, median, skewness, kurtosis, and standard deviation	45
Lung Biomechanical	1. Jacobian 2. Strain 3. Deformation Index (ADI)	mean, median, skewness, kurtosis, and standard deviation	15

Table 3: Complete feature calculation information

3.5.1. Density Based Feature Set

Density based feature set consists of measure for the extent of emphysema and air trapping in a COPD subject. The densitometry measures are computed from the entire lung fields and also from the lobes. These measures correspond to the amount of voxels below a given HU threshold relative to voxels in the whole lung. Emphysema is calculated from the inspiration image and a threshold of -950HU is used [8]. Similarly, air trapping extent is computed from the expiration image and a threshold of -856HU is used[9-11, 43]. These thresholds have been proven effective in quantifying the extent of emphysema and air trapping in COPD subjects.

3.5.2. Texture Based Feature Set

In order to capture the textural patterns, a set of 45 features that includes 3 local image descriptors computed at 3 different scales, are used. The detailed information of the filters is shown in table 4. The local image descriptors are based on the gaussian function and its rotationally invariant derivatives. The three different scales (standard deviation) represents the amount of smoothing for the gaussian kernel.

The following is the detailed descripiton of the filter bank,

1. *Convolution with Gaussian:*

    The feature images are computed by convolving it with the gaussian kernel at 3 different scales. This filtering technique blurs the images and reduces the noise. The gaussian function uses the following equation for the transformation.

$$G(x,y,z) = \frac{1}{2\pi\sigma^2} \exp(-\frac{|x|^2 + |y|^2 + |z|^2}{2\sigma^2}), -\infty < x,y,z < \infty$$

Image Descriptor	Feature Image	Equation
Smoothing	Convolution with Gaussian	(L = I *G)
Rotationally invariant edge descriptor	Gradient magnitude	$L = sqrt(L_x^2 + L_y^2 + L_z^2)$
Rotationally invariant edge descriptor	Laplacian of the Gaussian	$(\lambda_1 + \lambda_2 + \lambda_3)$

Table 4: Gaussian filter bank calculated at 3 different scales used to form texture based feature set with the corresponding equations assuming $\lambda_1 \geq \lambda_2 \geq \lambda_3$

2. *Gradient Magnitude of the Gaussian*

This filter is used to determine the object contours and seperations, i.e. for edge detection in the images. It is derived by computing partial derivatives of the image,

$$Gradient\ Magnitude = \sqrt{(\frac{\partial I}{\partial x})^2 + (\frac{\partial I}{\partial y})^2 + (\frac{\partial I}{\partial z})^2}$$

3. *Laplacian of the Gaussian*

Laplacian operator computes the second spatial derivative of an image. It captures the regions of rapid intensity changes and is used in edge detection. To get the horizontal, vertical and depth information of the edges, we take the second derivative in x, y and z directions. Thus, the laplacian of the image is given by

$$Laplacian \; (\, \nabla^2 I \,) = \frac{\partial^2 I}{\partial x^2} + \frac{\partial^2 I}{\partial y^2} + \frac{\partial^2 I}{\partial z^2}$$

These three filters were calculated at three different standard deviation values (1.2, 2.4 and 4.8mm) giving 9 filtered versions for each expiration image in the dataset. We have calculated five first order statistical features: mean, median, skewness, kurtosis and standard deviation for nine filtered versions of each image. Therefore, a total of 45 features were computed to form a texture based feature set.

3.5.3. Lung Biomechanical Feature Set

This feature set is comprised of features which captures the lung function by non-rigid image registration of a pair of scans at different inflation levels. Mechanical analysis on a regional level is done by finding out the local tissue deformation pattern from the correspondence of each voxel between inspiration and expiration image. Three measures are calculated from this analysis:

- Jacobian
- Strain information and
- Anisotropic Deformation Index (ADI)

Jacobian

This feature measures the local volume change under deformation from the inspiration to expiration registration procedure. The Jacobian determinant is a measurement to estimate the point wise volume expansion and contraction during the deformation[19, 41]. In a three dimensional space, Let $h(x) = [h_1(x), h_2(x), h_3(x)]^T$ be the vector transformation and $u(x) = [u_1(x), u_2(x), u_3(x)]^T$ represents the deformation fields. The relationship between $h(x)$ and $u(x)$ is shown as $h(x) = x + u(x)$. The Jacobian of transformation J (h(x)) at $x = (x_{1,}x_{2,}x_3)^T$ is defined as

$$J\big(h(x)\big) = \begin{vmatrix} 1 + \dfrac{\partial u_1(x)}{\partial x_1} & \dfrac{\partial u_2(x)}{\partial x_1} & \dfrac{\partial u_3(x)}{\partial x_1} \\ \dfrac{\partial u_1(x)}{\partial x_2} & 1 + \dfrac{\partial u_2(x)}{\partial x_2} & \dfrac{\partial u_3(x)}{\partial x_2} \\ \dfrac{\partial u_1(x)}{\partial x_3} & \dfrac{\partial u_2(x)}{\partial x_3} & 1 + \dfrac{\partial u_3(x)}{\partial x_3} \end{vmatrix} \qquad (3.9)$$

The Jacobian at a given point gives important information about the transformation h near that point [44, 45]. If the Jacobian value is zero at x, then the transformation h is not invertible. If the Jacobian value is negative, then transformation reverses orientation. A positive jacobian preserves the orientation. Using a Lagrangian reference frame, the indications of Jacobian value are,

$$\begin{bmatrix} J > 0, \text{ preserve orientation} \begin{cases} J > 1, \text{ local expansion} \\ J = 1, \text{ no deformation} \\ 0 < J < 1, \text{ local contraction} \end{cases} \\ J = 0, \text{ non-injective} \\ J < 0, \text{ reverse orientation} \end{bmatrix}$$

Strain Analysis

Deformation patterns are characterized by the regional distribution of a strain or stretch tensor by the displacement fields from the registration process. A displacement gradient tensor u can be calculated as the partial differentiation of the displacement vector with respect to the material coordinates.

$$
\nabla u = \begin{vmatrix} \dfrac{\partial u_x}{\partial x} & \dfrac{\partial u_x}{\partial y} & \dfrac{\partial u_x}{\partial z} \\ \dfrac{\partial u_y}{\partial x} & \dfrac{\partial u_y}{\partial y} & \dfrac{\partial u_y}{\partial z} \\ \dfrac{\partial u_z}{\partial x} & \dfrac{\partial u_z}{\partial y} & \dfrac{\partial u_z}{\partial z} \end{vmatrix} \qquad (3.10)
$$

By applying strain tensor on the deformation gradient, the distribution of stress in the lung can be calculated. Linear strain along $x, y \ and \ z$ axes are defined as

$$
\varepsilon_x = \frac{\partial u_x}{\partial_x}, \varepsilon_y = \frac{\partial u_y}{\partial_y}, \varepsilon_z = \frac{\partial u_z}{\partial_z}. \quad (3.11)
$$

Where $u = [u_x, u_{y,} u_z]^T$ is the 3D displacement field. The concept of the strain is used to evaluate how much a given displacement differs locally from a rigid body displacement [46]. The strain tensors are represented as orthogonal eigenvectors by single value decomposition method. The maximum eigenvalue for each tensor is called maximum principle strain. Strain analysis gives valuable information about the directionalities in local tissue deformation.

Anisotropic Deformation Index (ADI)

Orientation preference also plays a role in the lung deformation in addition to the volume change[47]. Some regions may undergo no volume change with significant deformation and vice versa due to the compensation effects of lung elasticity. Anisotropic deformation index calculates the ratio of length in the direction of maximal extension to

the length in the direction of minimal extension. This index is calculated by decomposing the deformation gradient tensor in to stretch and rotational component.

$$F = \begin{vmatrix} 1 + \dfrac{\partial u_1(x)}{\partial x_1} & \dfrac{\partial u_2(x)}{\partial x_1} & \dfrac{\partial u_3(x)}{\partial x_1} \\ \dfrac{\partial u_1(x)}{\partial x_2} & 1 + \dfrac{\partial u_2(x)}{\partial x_2} & \dfrac{\partial u_3(x)}{\partial x_2} \\ \dfrac{\partial u_1(x)}{\partial x_3} & \dfrac{\partial u_2(x)}{\partial x_3} & 1 + \dfrac{\partial u_3(x)}{\partial x_3} \end{vmatrix} = RU \qquad (3.12)$$

Where R is the rotational tensor and U is the stretch tensor.

The Cauchy-green deformation tensor is defined as

$$C = FF^T = R^T U^T R U = U^T U \qquad (3.13)$$

To obtain the stretch information from U, Eigen decomposition of C is done. After taking the square root of eigenvalues of C, we get the eigenvalues of U which are principal stretches. The ratio of maximum eigenvalue over the minimum gives the regional stretch information, which represents anisotropic deformation index [31]. The value of ADI is always greater than or equal to one. If the value is close to one, it means there is an isotropic expansion and if the value is big, it represents anisotropic deformation.

3.6. Feature Selection

Feature selection plays a major role in building robust classification models by selecting a subset of best features. Feature selection algorithms are of two categories: feature ranking and subset selection. Feature ranking ranks the given set of features and eliminates the low ranked features to form an optimal set of features. Subset selection searches for the set of optimal features through various combinations of the given

features. The elimination of irrelevant and redundant features improves the performance of the classification. It speeds up the run time of the classification and reduces the curse of dimensionality. In this study, 62 features were calculated from three different feature calculation strategies. The selection of optimal features from each feature set, which can define the disease better than the other features, is possible through the feature selection process. Linear forward feature selection technique is used in this study to improve the classifier performance and also to test the effectiveness of the features in different classification experiments.
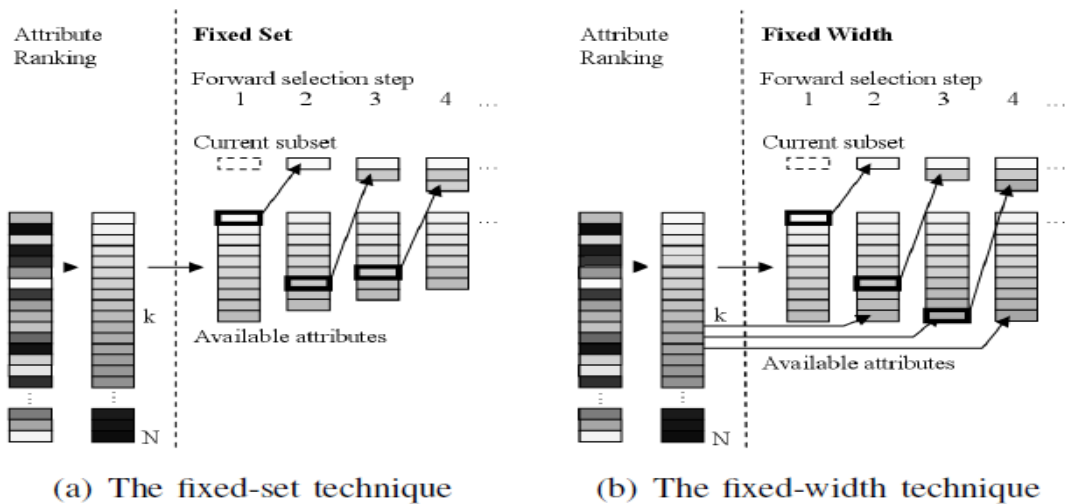
Figure 6: Linear forward selection algorithm. The first column in figure (a) and (b) shows the ranking of attributes represented by different colors. In the second column of (a) and (b), the features are arranged according to their rank. In the third column, fixed set technique, fig (a), selects the top k features and only these k attributes are used for subsequent selection process reducing the number of evaluations and eliminating irrelevant features at each step. In the third column, Fixed width technique, fig (b), selects the top k features and replaces with the next best attribute in the subsequent selection process. It maintains a fixed width in all the steps by taking low ranked attributes also into account. Adapted from [48, 49]

Linear forward selection is the modified version of the standard search technique known as sequential forward selection [48, 49]. Sequential forward selection is a hill climbing search which adds the feature that gives the best score to the optimal subset at each forward step. The search terminates when there is no improvement in the score with the remaining features. In this method, there will be a reduction in the number of features in each step of the forward search. The number of evaluations at each step is equal to the number of remaining features. The feature dependent evaluations reduce the run time performance of the algorithm and it can be problematic for high dimensional datasets. In the linear forward selection, user will be able to limit the number of features that are considered in each step and it significantly reduces the number of evaluations and run time [48].

There are two methods used by linear forward selection to limit the number of features: Fixed Set and Fixed Width, shown in figure 6. In fixed set, only the given features are ranked according to their scores by evaluating each feature individually. Only the k best features are selected for the next forward selection step. It discards most of irrelevant features and it reduces the number of evaluations drastically by selecting the given features to fixed set of size k. The subset of best ranked features increases at each forward step and the subset extension decreases with the each step. In fixed width, similar ranking of features is done as the fixed set method. However, at each forward step, the next best feature in the initial ranking is added to the subset by ensuring the subset with the individually best k features that have not been selected so far. Fixed width takes the weaker features into account as the search proceeds and the subset extension will be fixed width throughout the search.

3.7. Classification (KNN Classifier)

We have performed five classification experiments in this study. In all the experiments, we have used the k nearest neighbor learning algorithm [49, 50]. K nearest neighbor algorithm is a non-parametric approach based directly on distances computed between training and test data points. It is a supervised pattern classification algorithm. It has been shown to work well in the classification of lung tissue[13, 14, 51, 52]. This classifier does not require any prior information about the distribution of the data points.
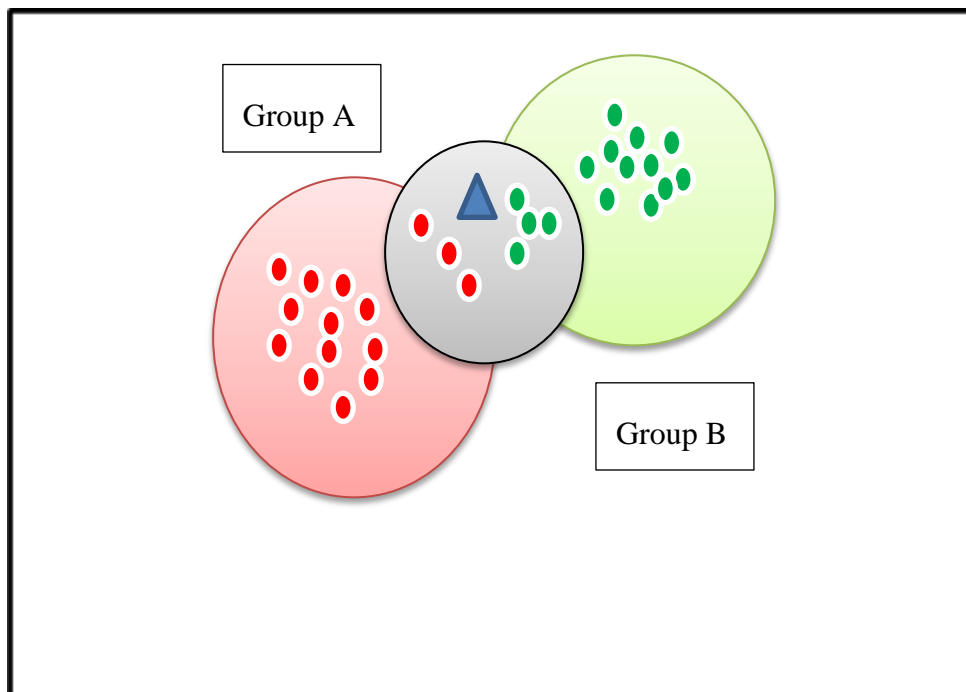
Figure 7: KNN classifier example

For any given test data point, KNN searches its nearest neighbors formed by the training data sets. The classifiers return the selected number of neighbors (k) which are closest in the distance to the given test data point. The choice of k is user defined and it defines the smoothness of the decision boundary. The decision is made based on the majority vote of its neighbors, with the test data point being assigned to the group most common among its nearest neighbors. The running time of KNN grows exponentially with n-dimensional space. As an example, in figure 7, there are 15 data points in group A (red), 15 in group B (green) and one test data point (blue). KNN computes the Euclidean distance to each data point in group A and group B from the test data point. In this example, the k value is chosen as 7. It selects 7 nearest neighbors closest to it based on the distance calculation. Since there are 4 data points from Group B out of 7 nearest neighbors, the given test data point is labeled as group B by the classifier. In this study, we have used instance based k nearest neighbor (IBk) learning model in WEKA machine learning framework to perform the k nearest neighbor search [49]. Euclidean distance method is followed to compute the distances between nearest neighbors.

CHAPTER 4

EXPERIMENTS AND RESULTS

4.1. Feature Calculation Results and Correlations with Pulmonary Function Test Measures

A total of 62 features from the CT images were used in this study. These features are categorized into three feature sets: Density based (2), Texture based (45) and lung biomechanical based (15). Density based feature set comprises of emphysema (percent below -950HU) and air trapping (percent below -856HU) measures. The emphysema and air trapping percentages of all the subjects in this study are shown in figure 8. Texture based feature set consists of features calculated from gaussian filtered versions of the expiration image at multiple scales. The gradient magnitude of gaussian and laplacian of gaussian filtered versions at scales 2.4mm for a nonsmoker subject and a GOLD4 COPD subject is shown in figure 9. Lung biomechanical feature set consists of features calculated from the registration of inspiration to expiration image. Three regional lung tissue estimates are used in this feature set: Jacobian, Strain and ADI. The Jacobian and Strain maps of a GOLD0 and a GOLD4 COPD subject are shown in figure 10.

As an initial step towards the classification of COPD subjects, correlations of CT derived features with PFT measures and COPD GOLD stage values were calculated. These correlation values provide the information on the relationship between CT derived features and the clinical diagnostic measures of the disease. Density based features showed good negative correlations, in particular, the air trapping measure (percent below -856HU) showed correlation greater than -0.8 with all the three measures. The Jacobian measure has the correlation of greater than 0.8 with PFT measures and -0.85 with the GOLD stage values. The texture based features also correlated well with coefficients ranging from 0.5 to 0.8. The number of features per feature set that showed either a

negative or positive correlation of 0.5 or high with the significance level of $p<0.05$ is shown in table 5.
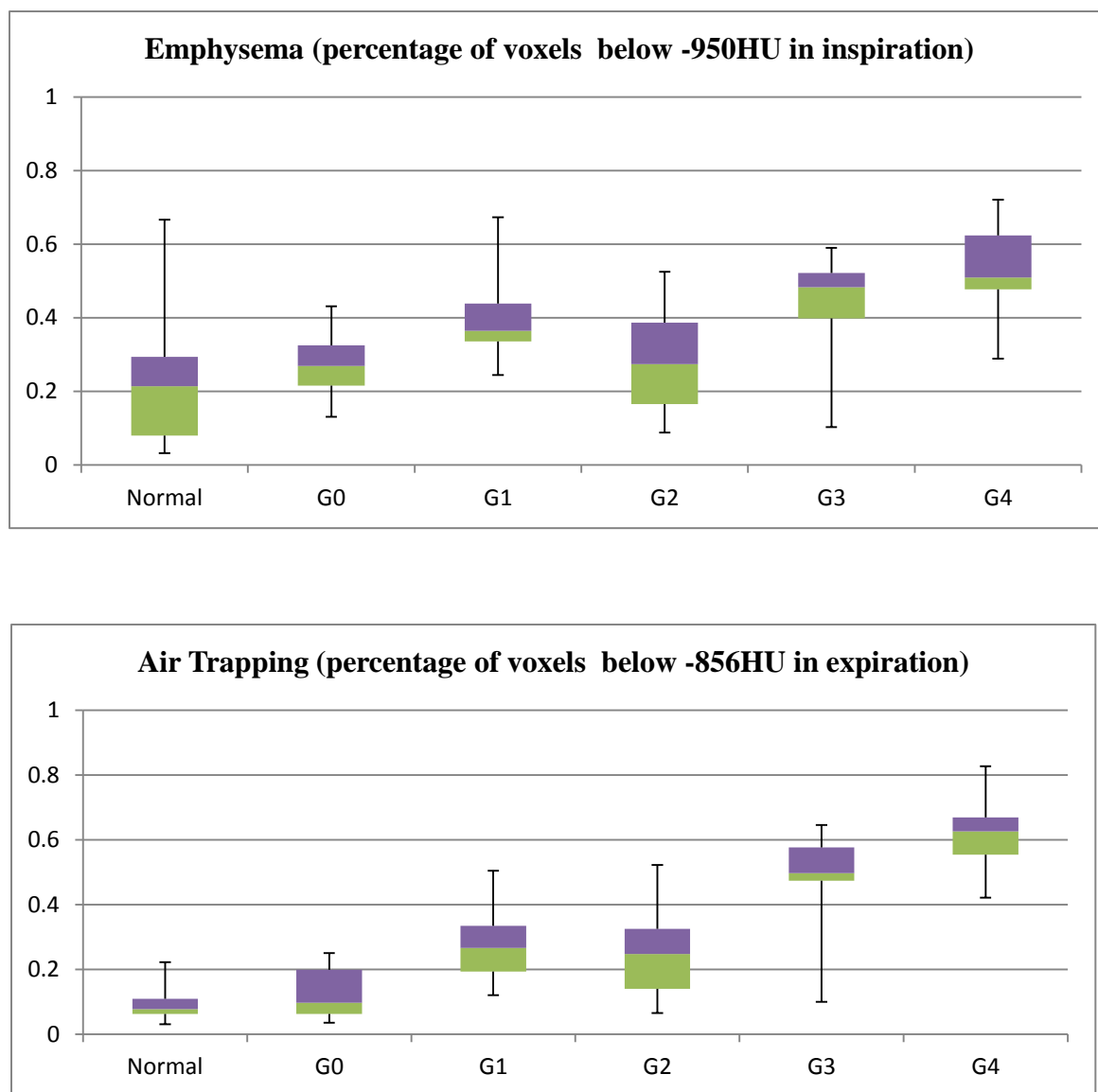
Figure 8: Boxplots showing the percentage distribution of emphysema and air trapping of all the subjects according to the GOLD stage. The two whiskers at both ends represent high and low values of the data. The box represents 50% of the values with 75th percentile as the top value and 25th percentile as the bottom value. The division in the middle represents median value (50th percentile)
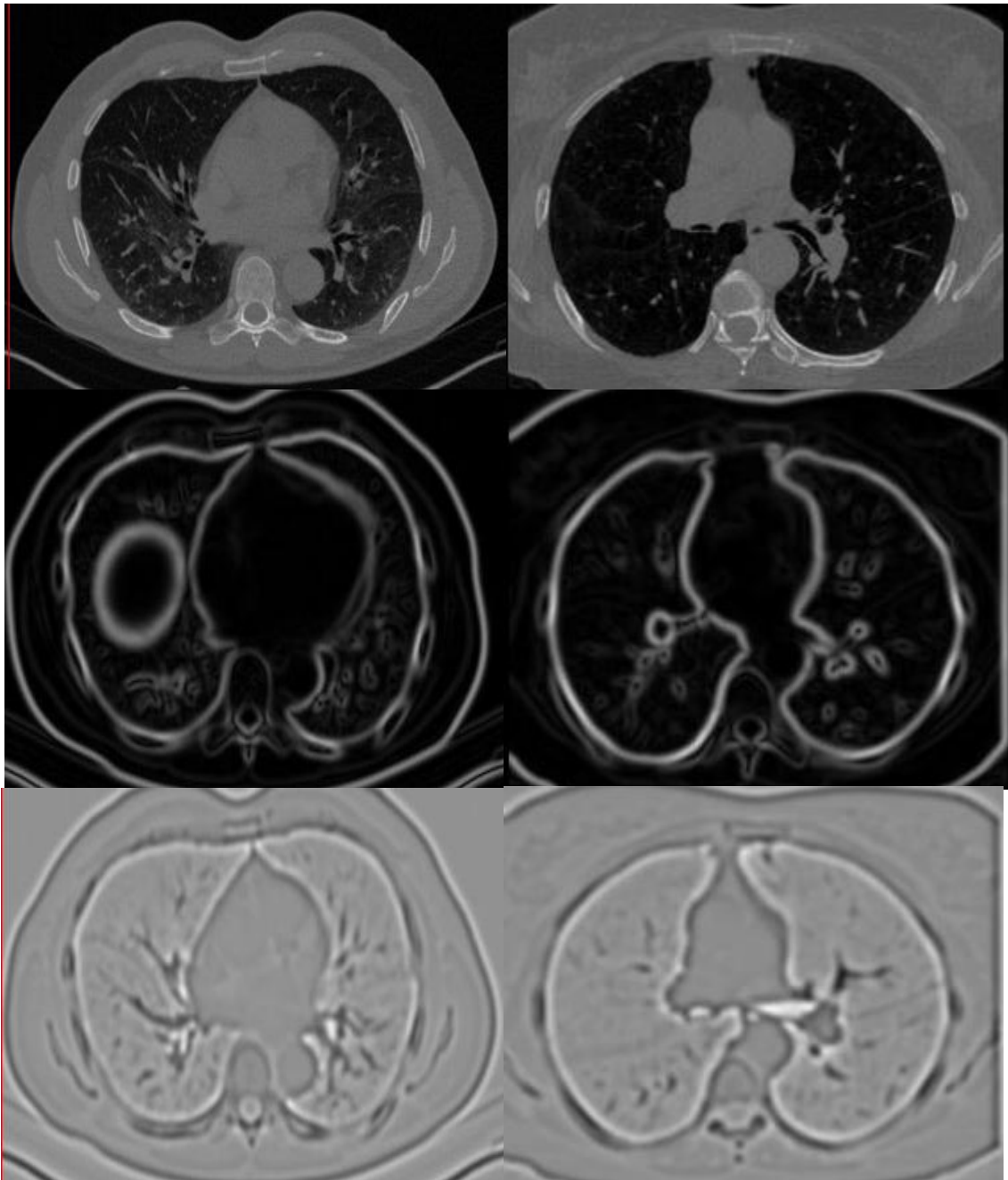
Figure 9: Axial slices of the original images (first row) with their corresponding gradient magnitude of gaussian filtered image (second row) and the laplacian of the gaussian image (third row) at 2.4mm standard deviation. First column represents nonsmoker subject and second column represents GOLD4 COPD subject
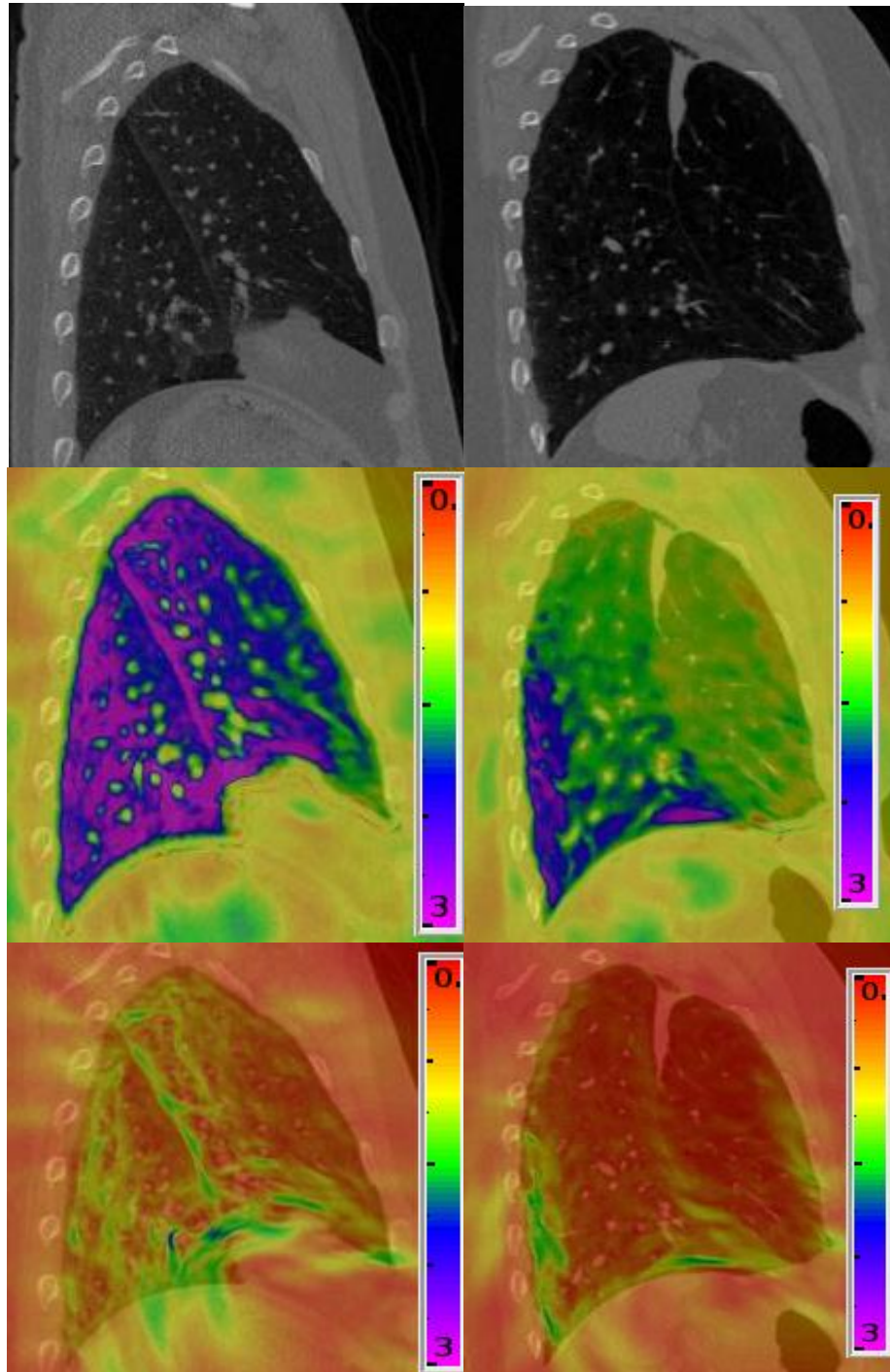
Figure 10: The Jacobian (second row) and Strain maps (third row) on the sagittal slice of the original FRC image (first row). First column represents GOLD0 COPD subject and the second column represents GOLD4 COPD subject.

FEATURE SETS	PFT MEASURES		
	FEV$_1$/FVC	*FEV$_1$% Predicted*	*GOLD Values*
Density Based (2)	2	2	2
Texture Based (45)	18	15	19
Lung Biomechanical (15)	10[*]	10[*]	10[*]

(*) values are statistically significant with $p < 0.0001$

Table 5: Number of features per feature set with a correlation coefficient of either (-0.5 to -1) or (0.5 to 1) with clinical PFT measures showing a statistical significance $p < 0.05$

The two density based features and ten lung biomechanical features showed good correlations with the three clinical measures. All the lung biomechanical features are found to be statistical significant with $p < 0.0001$ significance level. Out of 45 features, a good number of texture based features also correlated well with the given measures. These correlations prove a definite relationship between the calculated features and the clinical diagnostic measures.

4.2. Classification Experiments

We have performed five classification experiments to classify COPD subjects from normal subjects and also to assess the disease progression at various stages. Three experiments are based on the features calculated from the whole lung and the remaining two experiments are based on the features from the lobes of a lung. Whole lung level experiments are performed to classify COPD subjects from the normal subjects and also

to classify COPD subjects to their corresponding severity stage. Lobar level experiments are used for regional level assessment of the disease in the lungs. The five experiments are as follows:

1. Severe COPD vs. Non COPD (Whole lung)
2. Mild to severe COPD vs. Non COPD (Whole lung)
3. Mild to severe COPD vs. Non COPD (Lobar level)
4. GOLD category classification (Whole lung)
5. GOLD category classification (Lobar level)

In addition to the three feature sets: density, texture and lung biomechanical, a new feature set is formed which is the combination of best features from each of the three feature sets. The fourth feature set is referred as ALL in the classification experiments. The best subset of features is selected by linear forward feature selection approach. Nearest neighbor algorithm is used for the classification and the optimal k value is selected by the cross validation technique. The dataset is divided in to test and training data using leave one out cross validation technique. In leave one out cross validation, one subject from the data set is used as a test data every time and the remaining subjects as the training data. The process is repeated such that every subject in the data is used as a test data for at least once.

To estimate the classifier performance in each experiment, the area under the receiver operator characteristic curve (ROC) measurement is used, often called AUC measure. AUC provides a single measure showing the probability that a classifier will rank a randomly chosen positive instance higher than a randomly chosen negative one. AUC value range from 0 to 1 with 0 being worse and 1 being the perfect classification. In addition to the AUC measure, a ROC curve estimating the performance of feature sets for each class label in the classification is shown. Multiple regression analysis is done to find

the correlation between the optimal features selected in the classification and PFT measurements ($FEV_1\%$ predicted and FEV_1/FVC). The adjusted R squared correlation coefficient, is reported from the regression analysis. Adjusted R squared coefficient uses the variances instead of variations which takes the sample size and number of predictor variables into consideration. The results of the experiments are shown in the order of materials and methods used for the experiment, ROC graphs for each class label in the classification, area under the curve (AUC) results of the classification with correlations between the PFT parameters and a table showing optimal features selected from each feature set.

4.2.1. Severe COPD vs. Non COPD (Whole Lung)

The initial experiment is designed to estimate the effectiveness of the proposed lung biomechanical feature set and the combination feature set (ALL) in distinguishing severe COPD and non COPD subjects. The results are compared with the density based and texture based features. The materials and methods followed in this experiment are shown in table 6. Two groups of data are considered for this experiment: The non-smoker subjects are considered as healthy cases and subjects from GOLD3, GOLD4 severity stage are considered as the diseased cases. Classification is done on 45 subjects with 15 nonsmokers and 30 severe GOLD stage subjects as explained in table 6.

All the four feature sets achieved almost 100% classification accuracy with an AUC of 0.99 in this experiment, as shown in table 7. Correlation between the optimal features from the feature sets and PFT parameters is shown in table 7. Density based and texture based features showed excellent correlations with FEV_1/FVC when compared to the correlations with $FEV_1\%$ predicted. The proposed lung biomechanical features showed correlations greater than 0.85 with both the PFT measures. When the best features from each feature set combined together in ALL, there is a significant

improvement in the correlations by maintaining the same classification accuracy. The optimal features selected for the classification are shown in table 8.

Classification	Non COPD vs. Severe COPD classification
Dataset	Non COPD, GOLD3, GOLD4 (15 subjects/case)
Total number of subjects	45 (15 Non COPD vs. 30 Diseased)
Feature sets	Density, Texture, Lung Biomechanical, ALL
Feature selection algorithm	Linear forward selection
Classification algorithm	K nearest neighbor , leave one out cross validation

Table 6: Material and Methods for experiment 4.2.1

Feature sets	AUC	Correlation FEV$_1$%	Correlation FEV$_1$/FVC
Density Based	0.99	0.79	0.91
Texture Based	0.98	0.71	0.88
Lung Biomechanical	0.99	0.85	0.86
ALL	0.99	0.87	0.92

Table 7: Area under the ROC curve and correlation results from multiple regression analysis for each feature set and all the reported correlations are statistically significant with $p < 0.0001$

Feature Set	Optimal Features
Density based	emphysema, air trapping
Texture based	gaussian, gradient magnitude of Gaussian
Lung biomechanical based	jacobian, Strain, ADI

Table 8: Optimal set of features selected for severe vs. normal classification where ADI represents anisotropic deformation index

The following observations can be made from this experiment:

1. There is a definite scope for the proposed lung biomechanical features in analyzing COPD. Inclusion of mechanical features to density and texture based features improved the overall performance of the system.

2. Density based features have a high correlation of 0.91 with the FEV_1/FVC, which is a clinical measure for the presence or absence of COPD.

3. Lung biomechanical features have good correlations with both the PFT measures, in particular, it showed excellent correlation with the severity measure $FEV_1\%$ predicted with a significance level of $p < 0.001$.

4. There is a significant increase in the correlation with PFT measures when all the feature sets combined together.

4.2.2. Mild to Severe COPD VS. Non COPD

(Whole Lung)

As a next step, the performance of lung biomechanical feature set and the combination feature set (ALL) in detecting the presence or absence of COPD is tested. The results are compared with the density based and texture based features. The materials and methods followed in this experiment are shown in table 9. The dataset is divided in to two classes for this experiment: nonsmokers, GOLD0 subjects as healthy cases and subjects from GOLD (1-4) stages are considered as diseased cases. A total of 90 subjects are used for this experiment considering 30 healthy and 60 diseased cases. ROC curves for normal and COPD subject classifications are shown in figure 11 and figure 12.

Classification	COPD vs. Non COPD classification
Dataset	Non COPD, GOLD0, GOLD1, GOLD2, GOLD3, GOLD4
Total number of subjects	90 (30 Normal vs. 60 Diseased)
Feature sets	Density, Texture, Lung Biomechanical and ALL
Feature selection algorithm	Linear forward selection
Classification algorithm	K nearest neighbor search, leave one out cross validation

Table 9: Dataset and algorithm information for experiment 4.2.2
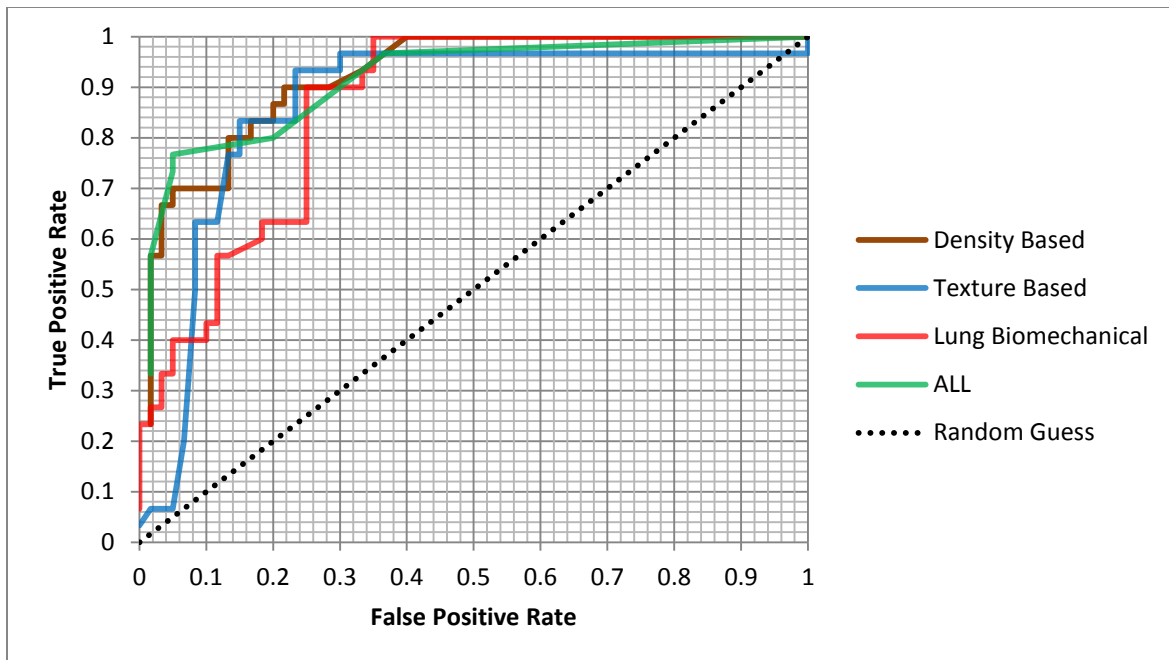
Figure 11: ROC curves showing the performance of the feature set in classifying healthy subjects
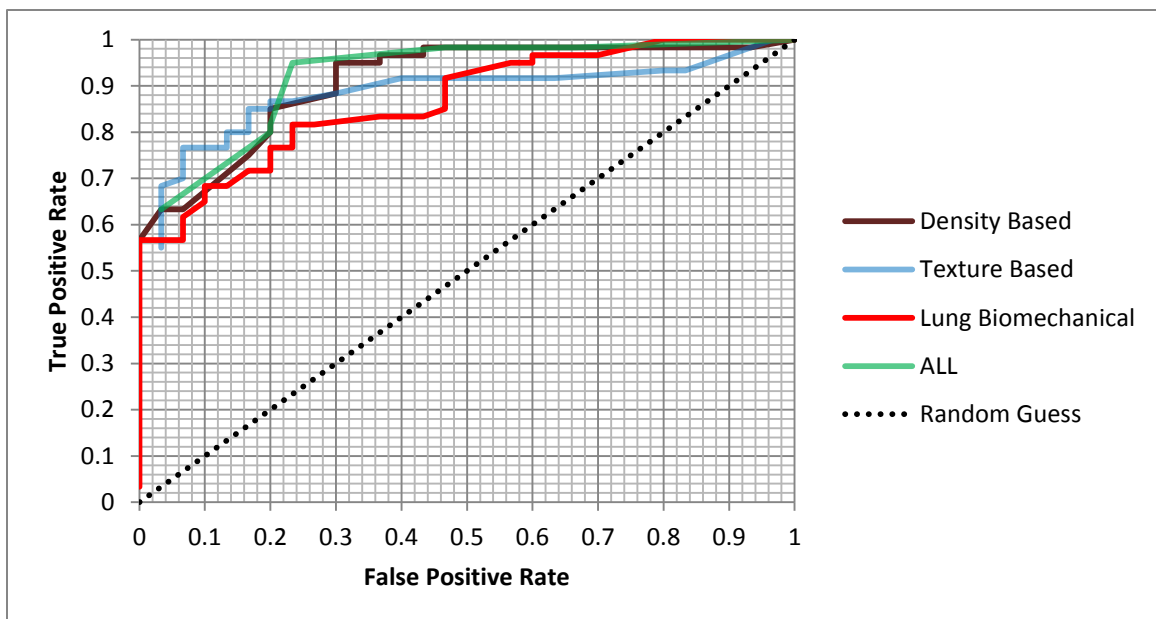
Figure 12: ROC curves showing the performance of the feature set in classifying COPD subjects

Density features were successful than the other feature sets in recognizing COPD. Density features achieved an AUC of 0.92 and correlated well with FEV_1/FVC measure as shown in table 10. Textural and mechanical features achieved an AUC of 0.86 (table 10). Textural features showed better correlation with FEV_1/FVC measure whereas lung biomechanical features correlated well with $FEV_1\%$. When the feature sets combined together in ALL, there is a significant improvement in the classifier performance. Also, better correlations with the PFT measures are observed.

Feature sets	AUC	Correlation FEV₁%	Correlation FEV₁/FVC
Density Based	0.92	0.71	0.85
Texture Based	0.86	0.66	0.77
Lung Biomechanical	0.86	0.74	0.71
ALL	0.92	0.82	0.85

All the correlations showed a statistical significance of $p < 0.0001$

Table 10: Area under the ROC curve for the whole lung COPD/Non-COPD classification and correlations with PFT measures from multiple regression analysis

The optimal features of each feature set from the feature selection process are shown in table 11. Jacobian features are selected from the lung biomechanical feature set. Both emphysema and air trapping are shown to be effective in detecting COPD presence. Features calculated from gradient magnitude of the gaussian and the laplacian of gaussian filters are the selected texture based features.

Feature Set	Optimal Features
Density based	emphysema, air trapping
Texture based	gradient magnitude and laplacian of the Gaussian
Lung biomechanical based	Jacobian

Table 11: Optimal set of features selected for COPD/Non-COPD classification.

Although density based features showed better classification accuracy in the overall COPD/Non-COPD classification, the percentage of COPD subjects that are classified as normal subjects using density features is high. Lung biomechanical features have a comparatively less error percentage than the density and texture features. A graph showing the true positive rate against the false negative rate for each feature set in COPD/Non-COPD classification is shown in figure 13. Texture based and density based features have shown higher error rate in classifying diseased subjects. Textural features have more than 50% misclassification of COPD subjects. When lung biomechanical features added to texture and density features, the percentage of false negatives is significantly decreased.

This experiment shows:

1. The strength of density based features in finding the presence or absence of COPD. This feature set achieved an AUC of 0.92 and a high correlation of 0.85 with FEV_1/FVC diagnostic measure.

2. Lung biomechanical features, in particular Jacobian measure, achieved an AUC of 0.86 in detecting COPD presence. Also, it showed good correlation of 0.73 with the severity measure $FEV_1\%$ predicted.
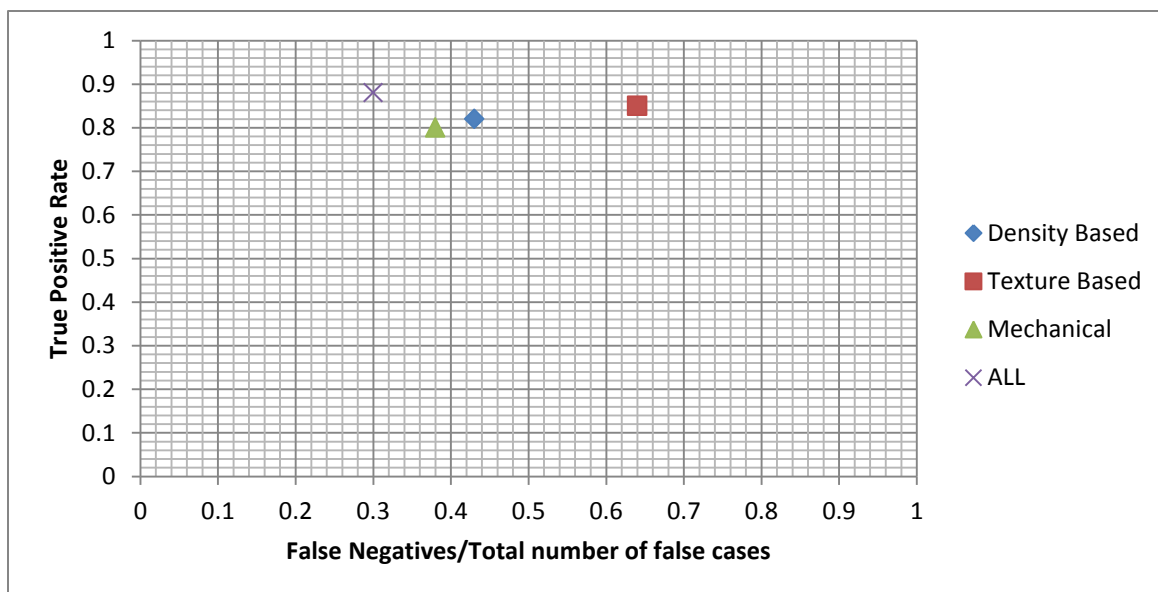
Figure 13: Graph showing the false negative rate in COPD/Non-COPD classification.

3. When the density, texture and mechanical features combined together, it achieved an AUC of 0.92 with significant improvement of correlation with both the PFT measures.

4. Lung biomechanical features and the combination of all the features showed less error percentage in classifying COPD cases.

4.2.3. Mild to Severe COPD VS. Non-COPD

(Lobar Level)

A two-class classification experiment is performed to detect COPD presence in lobes of the lung. Classification is performed using the features calculated from upper lobes and lower lobes separately. The disease label is assigned to a lobe from the label of the whole lung for training purposes. If the subject falls into a GOLD category, then all the lobes of the lung are assigned with same GOLD label. The dataset is divided into 30 normal cases and 60 diseased cases. The classification is performed to check how well the proposed feature sets can classify lobes into a disease or a normal class. The three feature sets: density based, texture based and lung biomechanical based are extracted from upper lobes and lower lobes separately. The methods and materials used in this experiment are shown in table 12. The area under the curve results of classification are shown in table 13 and 14. The ROC plots for lower lobe and upper lobe classification of COPD/Non-COPD are shown in figure 14, 15, 16 and 17. The optimal features selected from each feature set in the lobar classification are shown in table 15.

Similar to the whole lung results, the combination feature set is the best of all feature sets in both upper lobe and lower lobe classification in detecting COPD presence. All the feature sets achieved better classification results in the lower lobe classification than the upper lobes. Density based features achieved an AUC of 0.92 at lower lobes by showing good correlation with the FEV_1/FVC measure, shown in table 13. Lung biomechanical features achieved an AUC of 0.85 at lower lobes and correlated well with both the PFT measures. All the feature sets have a poor correlation with $FEV_1\%$ predicted in the upper lobe classification, shown in table 14. Texture based features performed well with an AUC of 0.86 at upper lobes. The classification accuracy is

significantly increased at upper lobes when all the features combined together. Also, the combination feature set showed better correlations with the PFT measures in the upper lobe classification. (Table 14)

Classification	Lobar analysis (COPD/Non-COPD classification)
Dataset	Normal, GOLD0, GOLD1. GOLD2, GOLD3, GOLD4 (15 subjects/case) divided into upper lobes, lower lobes
Total number of subjects	90 (30 Normal/GOLD0 vs. 60 GOLD1-GOLD4)
Feature sets	Density, Texture-based, Lung Biomechanical, All
Feature selection algorithm	Linear forward selection
Classification algorithm	K nearest neighbor search, leave one out cross validation

Table 12: Material and Methods for Experiment 4.2.3
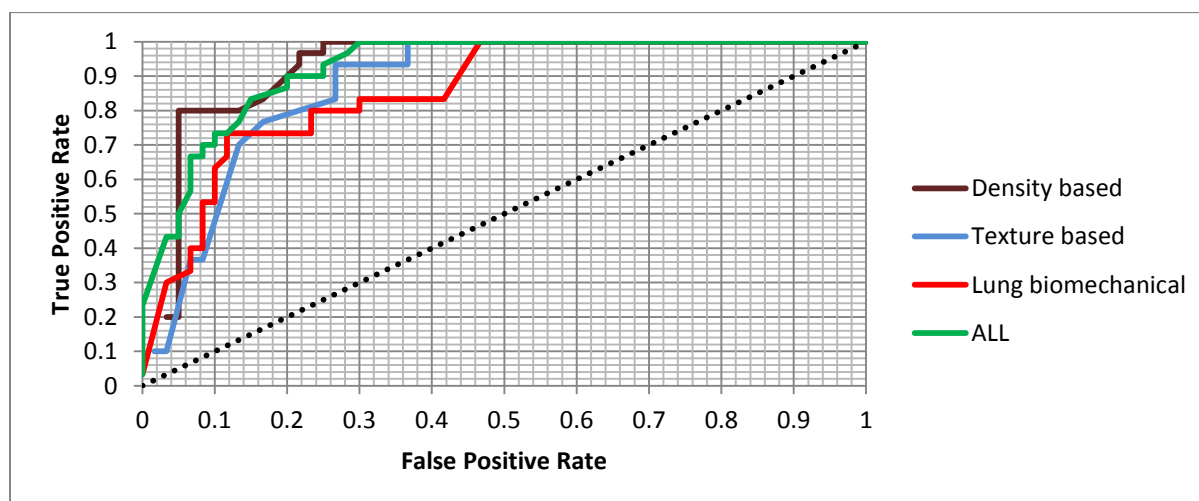
Figure 14: ROC curves showing the performance of the feature sets in classifying lower lobes of Non – COPD subjects
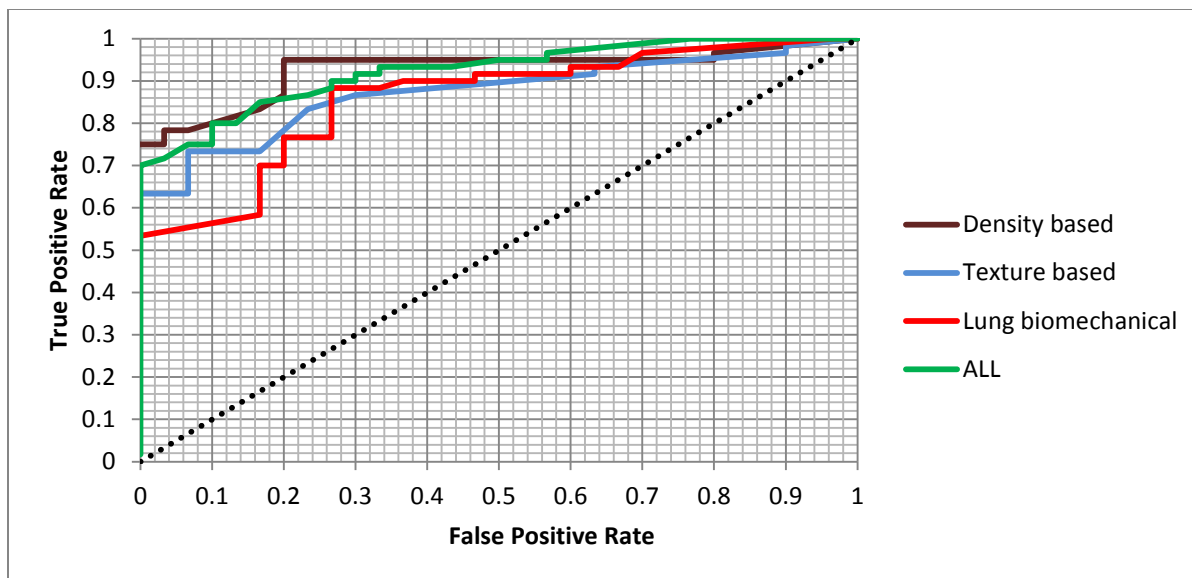
Figure 15: ROC curves showing the performance of the feature sets in classifying lower lobes of COPD subjects

Feature sets	AUC	Correlation FEV$_1$%	Correlation FEV$_1$/FVC
Density Based	0.92	0.61	0.72
Texture Based	0.87	0.60	0.75
Lung Biomechanical	0.85	0.74	0.77
ALL	0.92	0.76	0.79

All the reported correlations showed a statistical significance of $p < 0.0001$

Table 13: Area under the ROC curve for the lower lobes and correlation results from multiple regression analysis for each feature set.

Figure 16: ROC curves showing the performance of the feature set in classifying upper lobes of non-COPD subjects
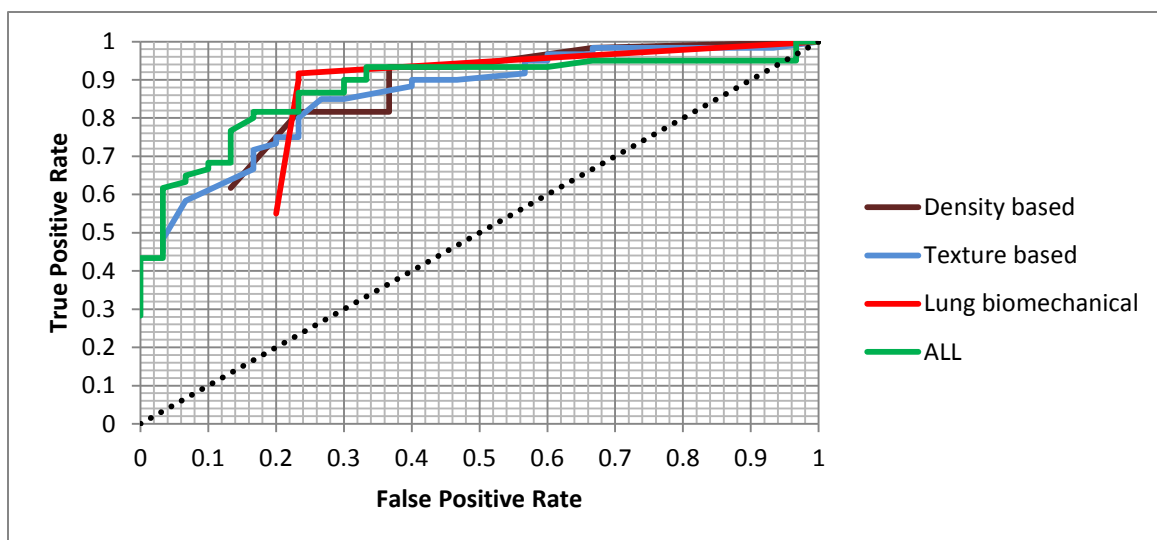
Figure 17: ROC curves showing the performance of the feature set in classifying upper lobes of COPD subjects

Feature sets	AUC	Correlation FEV$_1$%	Correlation FEV$_1$/FVC
Density Based	0.83	0.59	0.72
Texture Based	0.86	0.59	0.71
Lung Biomechanical	0.81	0.56	0.61
ALL	0.88	0.65	0.74

All the correlations showed a statistical significance of $p < 0.0001$

Table 14: Area under the ROC curve for the upper lobes and correlation results from multiple regression analysis for each feature set.

Feature Set	Upper lobes	Lower lobes
Density based	air trapping	air trapping
Texture based	gaussian, gradient magnitude, and laplacian of the gaussian	gaussian, gradient magnitude, and laplacian of the gaussian
biomechanical based	jacobian, strain	jacobian, strain, and ADI

Table 15: Optimal set of features selected for lobar level COPD/Non-COPD classification.

The following observations can be made from this experiment:

1. The higher classification accuracies at the lower lobes demonstrating the greater influence of airflow obstruction than at the upper lobes.

2. The better correlations of lung biomechanical features with the pulmonary function measures at lower lobes indicate more lung functional changes happening in this region.

3. Inclusion of lung biomechanical features to the density and textural features increase the classification accuracy in classifying upper lobes and lower lobes.

4. The combination feature set, ALL achieved better correlations with PFT measures from both upper lobe and lower lobe features.

4.2.4. GOLD Category Classification
(Whole Lung Level)

As a final step in the whole lung analysis, classification of COPD subjects into their corresponding GOLD severity stage based on the CT derived features is done. The dataset for this experiment comprises of 75 subjects with 15 subjects from each severity stage. It is a five class classification experiment given the GOLD severity range from 0 to 4. The materials and methods followed in this experiment are shown in table 16. ROC curves for each feature set performance at the five severity stages are plotted separately in figures 18, 19, 20, 21 and 22. Classification and correlation results are shown in table 17. The optimal features selected in the feature selection are shown in table 18. Air trapping measure is selected for severity classification from density based features. Features from all the three mechanical measures are selected from lung biomechanical feature set.

Lung biomechanical features are more effective in COPD severity assessment than the density and texture based features. Lung biomechanical features achieved an AUC of 0.80 and also correlated well with the FEV_1% predicted measure (Table 17). Density based features are shown to be highly correlated with the FEV_1/FVC measure. The combination feature set, ALL is the best of all feature sets by achieving a significant AUC of 0.86, shown in table 17. Also, there is a better correlation with the PFT measures with the ALL feature set.

|	
Classification	GOLD category classification
Dataset	GOLD0, GOLD1. GOLD2, GOLD3, GOLD4
Total number of subjects	75 (15 subjects/class)
Feature sets	Density-based, Texture-based, Lung Biomechanical, ALL (best feature subset)
Feature selection algorithm	Linear forward selection
Classification algorithm	K nearest neighbor , leave one out fold cross validation

Table 16: Material and Methods for Experiment 4.2.4.

Feature sets	AUC	Correlation FEV$_1$%	Correlation FEV$_1$/FVC
Density Based	0.78	0.69	0.83
Texture Based	0.77	0.63	0.72
Lung Biomechanical	0.80	0.72	0.66
ALL	0.86	0.84	0.84

All the correlations showed a statistical significance of $p < 0.0001$

Table 17: Area under the ROC curve and correlation results from multiple regression analysis for each feature set.
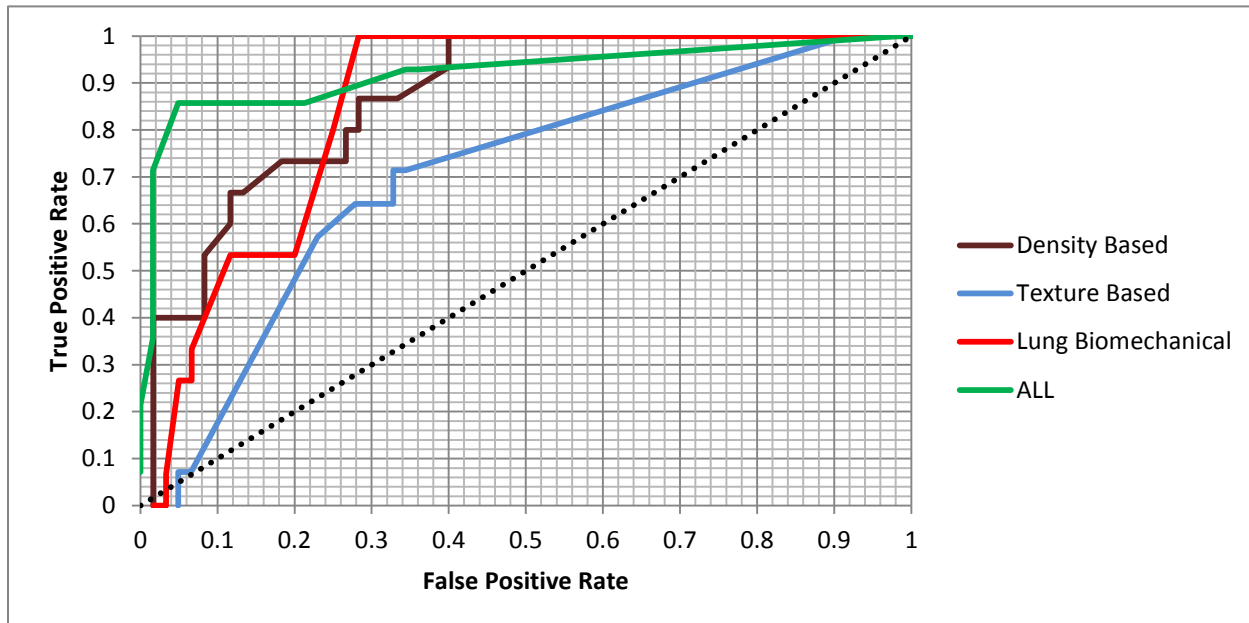
Figure 18: ROC curves showing the performance of the feature sets in classifying GOLD0 COPD subjects
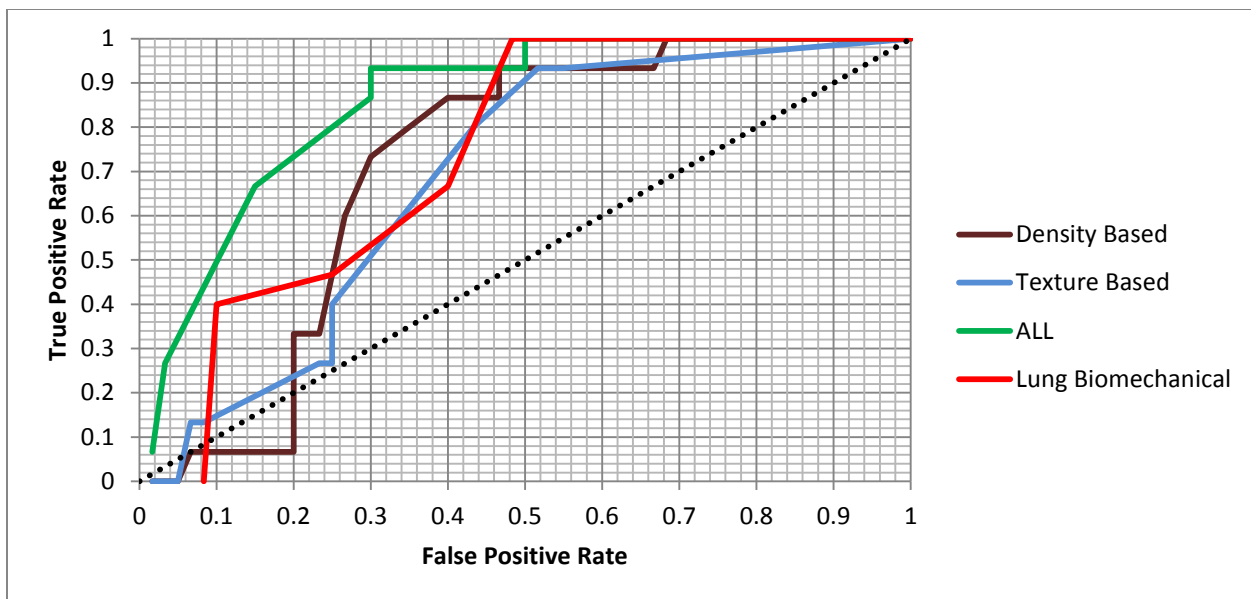
Figure 19: ROC curves showing the performance of the feature sets in classifying GOLD1 COPD subjects
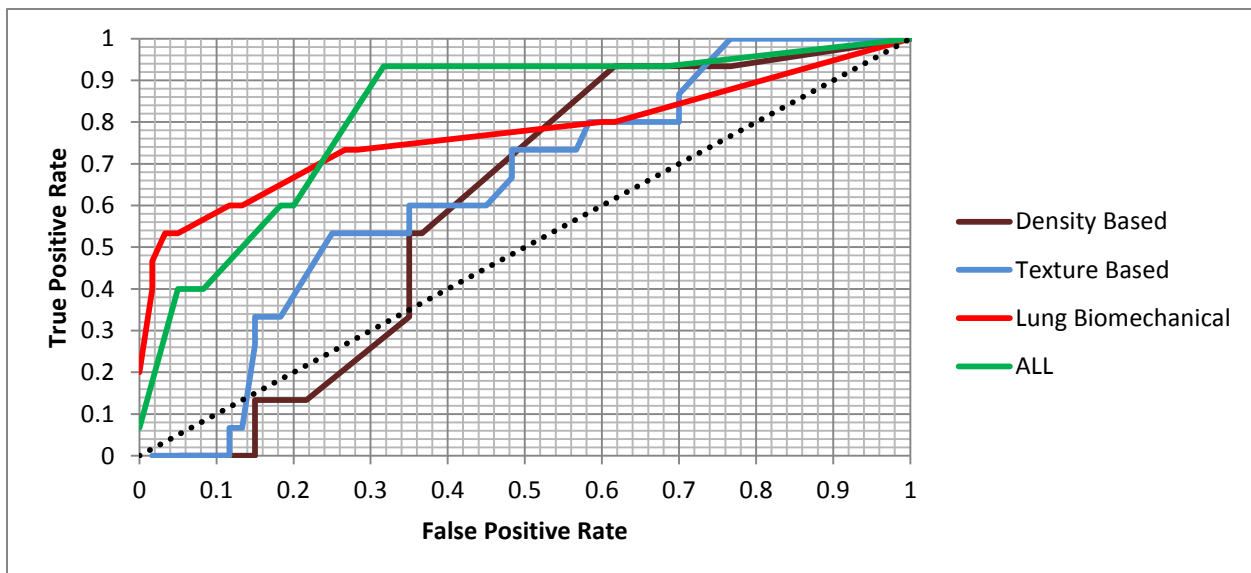
Figure 20: ROC curves showing the performance of the feature sets in classifying GOLD0 COPD subjects

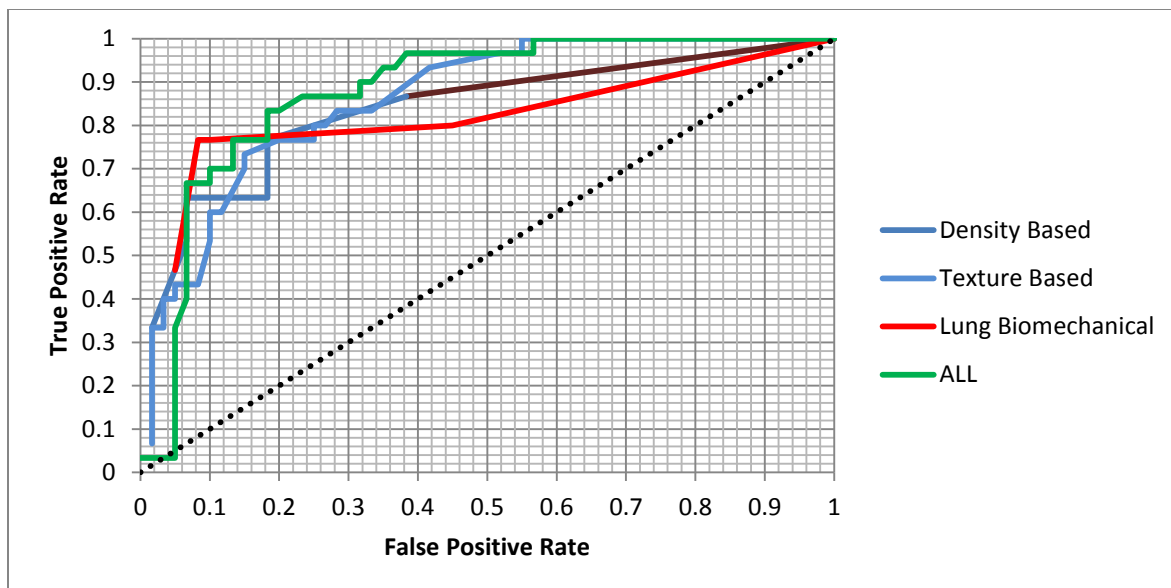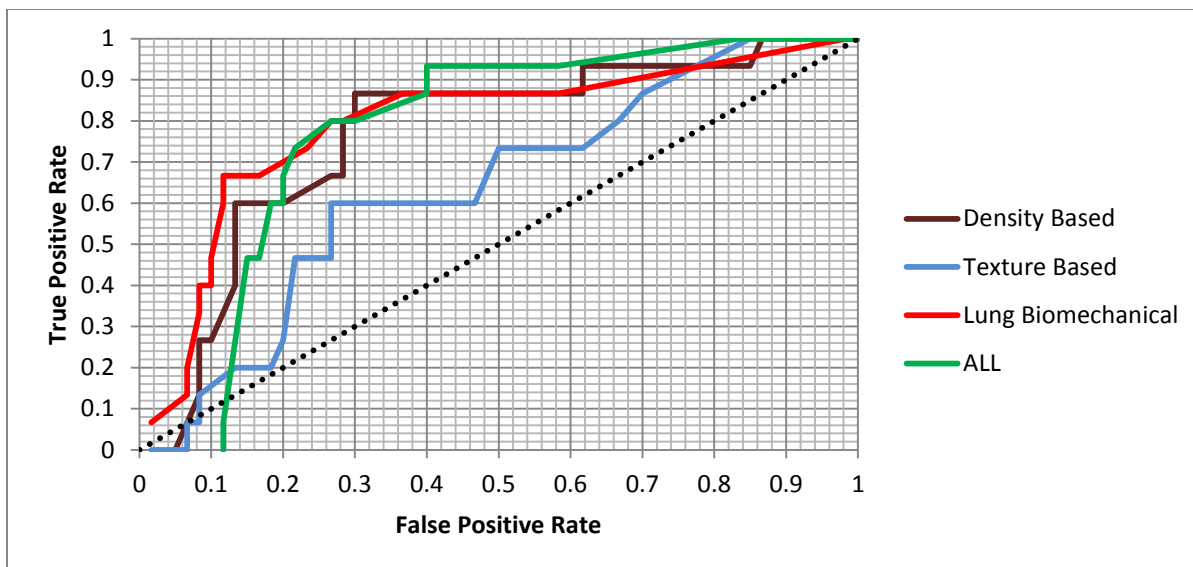Figure 21: ROC curves showing the performance of the feature sets in classifying GOLD3 COPD subjects
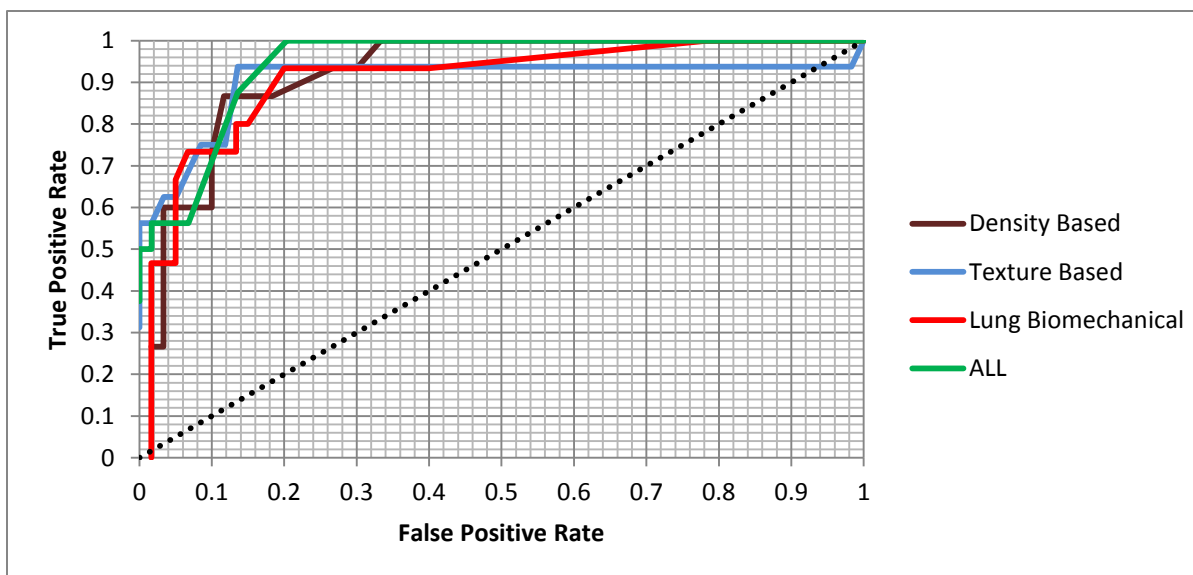
Figure 22: ROC curves showing the performance of the feature sets in classifying GOLD4 subjects.

Feature Set	Optimal Features
Density based	air trapping
Texture based	gaussian, gradient magnitude and laplacian of the gaussian
Lung biomechanical based	jacobian, Strain, ADI

Table 18: Optimal features selected for GOLD severity classification.

Lung biomechanical features have a higher rate of classification at the later stages of the disease than at the initial stages. In particular, at GOLD2 stage, density features and texture features failed to perform (figure 20). The confusion matrix of density, texture and mechanical feature sets in GOLD category classification is shown in table 19, 20 and 21.

	GOLD0	GOLD1	GOLD2	GOLD3	GOLD4
GOLD0	11	4	0	0	0
GOLD1	5	4	3	3	0
GOLD2	6	7	0	2	0
GOLD3	1	1	0	9	4
GOLD4	0	0	0	7	8

Table 19: Confusion matrix of density based feature set from the GOLD category classification of whole lung.

	GOLD0	GOLD1	GOLD2	GOLD3	GOLD4
GOLD0	8	2	3	1	0
GOLD1	2	10	3	0	0
GOLD2	4	7	1	3	0
GOLD3	1	2	1	11	0
GOLD4	0	0	0	6	9

Table 20: Confusion matrix of texture based feature set from the GOLD category classification of whole lung.

	GOLD0	GOLD1	GOLD2	GOLD3	GOLD4
GOLD0	11	4	0	0	0
GOLD1	11	2	1	1	0
GOLD2	3	1	9	1	1
GOLD3	0	1	2	9	3
GOLD4	0	1	0	5	9

Table 21: Confusion matrix of lung biomechanical feature set from the GOLD category classification of whole lung.
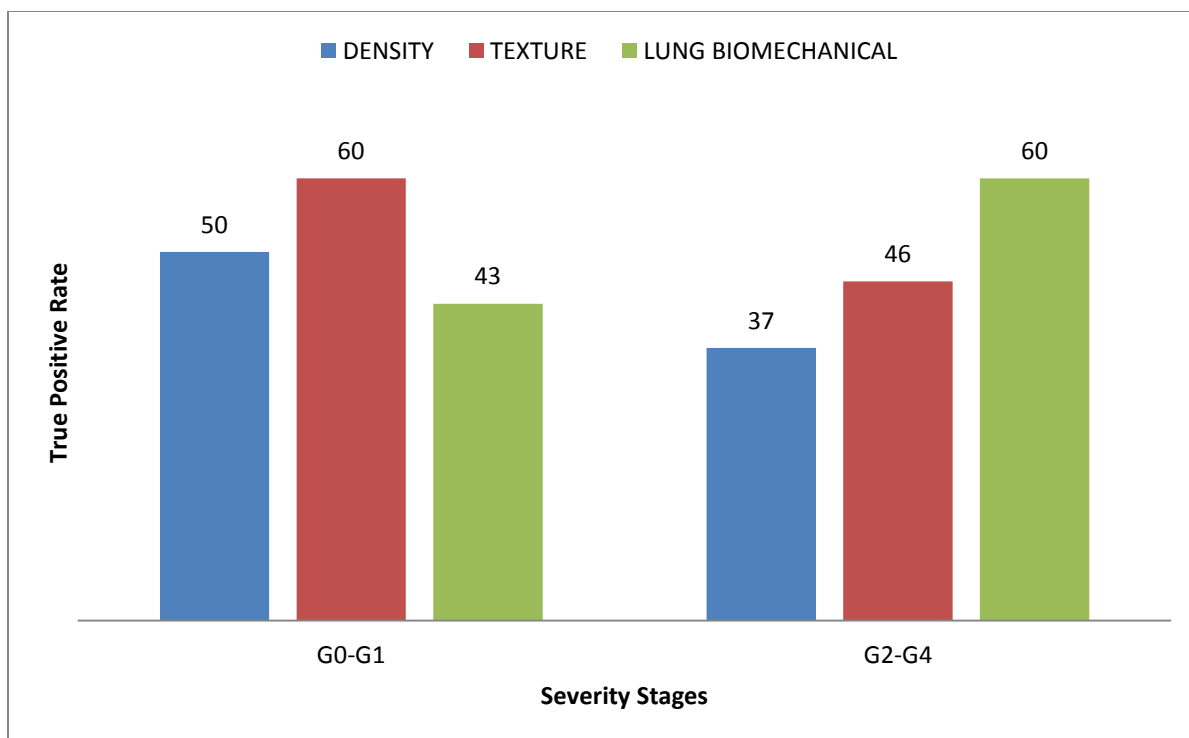
Figure 23: Chart showing the percentage of correctly classified instances at initial stages of the disease versus later stages of the disease. G0-G1 represents classification of GOLD0, GOLD1 subjects and G2-G4 for GOLD2, GOLD3, and GOLD4.

Density and texture based features together classified one GOLD2 subject correctly whereas 9 out of 15 GOLD2 subjects are identified by the lung biomechanical features, shown in table 19, 20 and 21. Density and texture based features have a better classification results at GOLD0 and GOLD1 stage. Lung biomechanical features showed difficulties in classifying GOLD1 stage subjects as most of them classified as GOLD0 stage. This suggests a possible onset of major mechanical changes in COPD subjects at GOLD2 stage. The classification accuracies of the three feature sets at the initial stages and later stages are shown in figure 23. Lung biomechanical features achieved higher accuracies from GOLD2 to GOLD4 stage where as texture based features have high classification rates at the initial stages.

This experiment shows:

1. The significant performance of the combination feature set with an AUC of 0.86 than the individual feature sets in the GOLD category classification.

2. Lung biomechanical feature performance with an AUC of 0.8, which is higher than the density based and texture based features. It also showed good correlation with FEV1% predicted measure.

3. Lung biomechanical feature classification accuracy is significantly higher at GOLD2 stage than the density and texture based features.

4. Density and texture based features higher correlations with FEV_1/FVC whereas lung biomechanical features have a good correlation with FEV_1% predicted.

5. Lung biomechanical features have higher classification accuracy at the later stages of the disease starting at GOLD2, which shows the onset of mechanical changes at that particular stage.

4.2.5. GOLD Category Classification (Lobar Level)

The progression of COPD at a regional level is estimated in this classification experiment. GOLD severity classification is done for upper lobes and lower lobes. The severity labels for lobes are assigned from the global label of the lung. The materials and methods used in this experiment are shown in table 22. AUC results for the classification of upper lobes and lower lobes are shown in table 23 and table 24.

Lung biomechanical features showed better classification results in assessing severity stage of the lobes. Higher classification accuracies and better correlations observed at the lower lobe classification than at the upper lobes. The combination feature set, ALL is the best of all with significant AUC of 0.75 and 0.84 at upper lobes and lower lobes. Also, there is a significant increase in the correlation with the PFT measures when all the feature sets combined. Lung biomechanical features showed better correlations

with the PFT measures at the lower lobes. Density based and texture based features have better correlation with FEV_1/FVC than the FEV_1 % predicted measure.

Classification	Lobar analysis (GOLD category classification)
Dataset	GOLD0, GOLD1. GOLD2, GOLD3, GOLD4 divided into upper lobes, lower lobes and the right middle lobe
Total number of subjects	75(15 subjects/class)
Feature sets	Density, Texture-based, Lung Biomechanical, All
Feature selection algorithm	Linear forward selection
Classification algorithm	K nearest neighbor, leave one out cross validation

Table 22: Material and Methods for Experiment 4.2.5

Feature sets	AUC	Correlation $FEV_1\%$	Correlation FEV_1/FVC
Density Based	0.69	0.59	0.66
Texture Based	0.72	0.58	0.69
Lung Biomechanical	0.74	0.55	0.57
ALL	0.75	0.62	0.70

All the correlations showed a statistical significance of $p < 0.0001$

Table 23: Area under the ROC curve for the upper lobes and correlation results from multiple regression analysis for each feature set.

Feature sets	AUC	Correlation FEV$_1$%	Correlation FEV$_1$/FVC
Density Based	0.75	0.59	0.69
Texture Based	0.73	0.57	0.70
Lung Biomechanical	0.76	0.75	0.75
ALL	0.84	0.77	0.79

All the correlations showed a statistical significance of $p < 0.0001$

Table 24: Area under the ROC curve for the lower lobes and correlation results from multiple regression analysis for each feature set.

CHAPTER 5

DISCUSSION

The conducted experiments in this study shows that the estimates of regional lung tissue expansion and contraction can be used to recognize COPD in pulmonary CT scans using supervised machine learning techniques. Density based features has been previously shown to be effective in COPD diagnosis[3, 7-9, 22, 23, 29, 53]. It also has been previously demonstrated that the textural patterns on CT images are useful in COPD classification[13-16, 33, 34]. In this study, the proposed lung biomechanical features are tested against these existing features for the classification of COPD. It is shown that the inclusion of mechanical features to the existing density based and texture based feature improves the detection of COPD presence and severity to a significant extent.

As an initial step in validating our proposed features, correlation of these features with the clinical pulmonary function test measures is checked. It is clear that all the lung biomechanical features are correlated to a good degree with the PFT measures. The jacobian measure showed excellent correlations of 0.83 and 0.84 with FEV_1/FVC, $FEV_1\%$ predicted values. However, jacobian measures comes after air trapping measure (percent -856) of the density based features, which showed high correlations of 0.83 and 0.91 with FEV_1/FVC, $FEV_1\%$ predicted values. All the correlation coefficients of the lung biomechanical features are found to be significant using t-tests with significance level $p < 0.0001$. This correlation with the PFT measures suggests a definite relationship between mechanical features and pulmonary function.

As a first classification experiment, a two-class problem was defined by the two subject groups, healthy (No COPD) and COPD (mild to severe) to estimate the performance of lung biomechanical features in recognizing COPD. The results of the classification are shown in table 10. The obtained lung biomechanical features compare well to previous methods in discriminating subjects with and without COPD, by

achieving an AUC of 0.86. Also, there is a good correlation of mechanical features with $FEV_1\%$ predicted values whereas density and textural features correlates best with FEV_1/FVC values. This suggests the sensitivity of mechanical features to the level of severity of the COPD, which is determined by $FEV_1\%$ predicted measure. When the proposed features combined with density and textural features, there is a significant increase in the classification accuracy and also in the correlation with $FEV_1\%$ predicted. Also, density based features achieved a better AUC of 0.92 in this experiment and showed good correlation of 0.85 with the FEV_1/FVC and 0.71 with $FEV_1\%$ predicted values. Despite of this good classification accuracy, density and textural features showed high misclassifications of COPD subjects as normal. On the other hand, lung biomechanical features have less misclassification rate resulting in overall rise of the classifier performance when all the feature sets combined together. This suggests that the mechanical features add important value in detecting COPD presence.

To assess COPD presence at a regional level, the same two-class problem was defined using the features calculated from upper lobes and lower lobes. We estimated the performance of proposed features in detecting COPD presence at the lobar level. The results from table 13 and 14 shows that all the features sets performed better at lower lobes than at upper lobes. Lung biomechanical features showed high correlations with PFT measures at lower lobes, showing its sensitivity to disease presence. Also, there is a significant improvement in the classification accuracy at upper lobes when all the features combined together. The combinations of features are observed to be more effective than the individual set of features in assessing COPD presence in upper lobes of the lung. Similarly, the combination resulted in better classification results at lower lobes. In these experiments at whole lung and lobar level, ten different mechanical features were selected for the classification. The jacobian measures are selected in both the whole lung and lobar classification whereas strain and ADI measures were selected for only lobar classification. This wide selection of different mechanical features shows the influence of

lung tissue deformational changes in regional assessment of COPD using pulmonary CT scans.

A five class problem was defined to categorize COPD subjects into their corresponding GOLD severity using the proposed mechanical features. Fifteen subjects from each GOLD severity were used. Lung biomechanical features are more effective than the density and texture based features in severity classification of COPD and correlated best with the severity measure, $FEV_1\%$ predicted values. Also, the inclusion of mechanical features to density and texture features resulted in a significant classification of COPD severity showing good correlations with the PFT measures. This shows the sensitivity of mechanical features to the COPD severity. One interesting observation from the severity classification results is the poor performance of density and texture features at GOLD2 stage of the disease. On the other hand, lung biomechanical features were able to classify nine out of 15 GOLD2 subjects compared to one subject with both density and texture combined. This suggests the possibility of major lung functional changes at GOLD2 stage, which were captured by lung biomechanical features. However, mechanical features were not able to differentiate GOLD0 and GOLD1 subjects. This is a possible indication of less mechanical changes in the lungs at initial stages of the disease. On the other hand, textural features were able to distinguish subjects better at the initial stages. These observations lead to a better classification accuracy at all stages of COPD when both textural and mechanical features combined together. The lobe by lobe analysis of COPD severity shows the higher classification accuracies at lower lobe. Lung biomechanical features achieved better AUC than the density and textural features and also significantly correlated with PFT measures. All the features calculated at upper lobes were poorly correlated with the PFT measures. With the combination of all the features, there is a significant increase in the classifier performance at both whole lung and lobar level severity classification. Also, the combination of features showed better correlations with the PFT measures. These results highlight the importance of adding mechanical

features to existing features for more accurate assessment of COPD severity. It is also important that these features can be measured at regional level of the lung, as opposed to PFT diagnosis based on whole lung function.

From the COPD/Non-COPD classification at both whole lung and lobar level, it must be noted, density and texture based features performed reasonably better than the lung biomechanical features. In particular, air trapping measure is proved to be a significant measure in detecting COPD presence. Since, the subject range in this classification is from GOLD1 to GOLD4 (mild to severe); there is a possibility of less lung functional changes happening at the initial stages. This leads to a higher number of misclassifications of GOLD1 as normal with lung biomechanical features, resulting in overall reduction of the classifier performance. However, in the classification of normal and severe COPD, the classification accuracy is same as density based and texture based features. This also suggests the effective performance of mechanical features at later stages of the disease. In addition to the density and texture based features that were used in this study, there are several other CT derived features which can be useful in more robust quantification of COPD. The number of features used in this study is less. There is a definite scope in testing the effectiveness of several other features either individually or in combination with the proposed features. The texture based feature set consists of three basic gaussian filtered versions of the image at multiple scales. There are other textural features which have been proven to be effective in COPD quantification[13-16]. Some of them are entropy, grey level non uniformities, co-occurrence matrices, run length matrices and other gaussian derivative filters. A complete system consisting of all the CT derived features related to both emphysema and small airway disease may result in more accurate measures of COPD.

The proposed features performed comparatively well with the previous methods of COPD diagnosis and severity classifications. The adaptive multiple feature method

(AMFM), proposed by Uppaluri et al., based on textural patterns of 2D CT images achieved an accuracy of 100% in classifying normal and severe emphysema subjects but with no significant correlation with PFT measures of emphysema[15]. The extension of 2D AMFM to 3D AMFM proposed by Xu et al. showed better results in discriminating normal smoker and nonsmoker lung parenchyma[16]. The combination feature set, ALL, also achieved significant classification rate at early stage discrimination of subjects. Another texture based approach proposed by Sorensen et al. based on gaussian filter versions of CT, achieved an AUC of 0.713 in classifying COPD and Non-COPD subjects[13]. The combination of registration based features with the density based features, proposed by Murphy et al. achieved an AUC of 0.92 in COPD diagnosis[27]. Recently, the combination of tracheal morphologic changes and emphysema features achieved an accuracy of 80% in GOLD0 versus GOLD1-4 classification[20]. In COPD diagnosis experiments, the combination feature set, ALL, achieved an AUC of 0.99 in normal versus severe COPD classification, an AUC of 0.92 in mild to severe COPD versus non-COPD classification showing significant correlations with PFT measures. In COPD severity classification, registration based ventilation measures proposed by Murphy et al. achieved 67% classification accuracy. The combination of tracheal changes with emphysema features achieved 51% accuracy[18, 20]. The proposed feature set, ALL, achieved an AUC of 0.86 in classifying COPD severity showing a significant correlation of 0.84 with both the PFT measures.

Accurate severity classification of COPD is difficult, due to many drawbacks associated with the PFT diagnosis, which is the sole measurement of severity. The major drawback is its reproducibility, which relies on the subject's ability to follow the given instructions on the day of diagnosis. A small error during the test may result in assigning different severity for the subject. There is a need to find the correlations of the proposed features with the diagnostic measures other than PFT. Some of them are St. George's Respiratory Questionnaire (SGRQ), modified Medical Research Council questionnaire

(mMRC), bode index of the subject, other measures of lung volumes and so on. Also, the size of the data used in this experiment is small (90 subjects) to conclusively state the results of this experiment. In the future, a larger number of subjects will be investigated.

COPD is a heterogeneous disease characterized by two components: chronic bronchitis and emphysema[1]. There are many other independent predictors of the disease and that COPD cannot be defined by a single measure. This results in different phenotype characteristics in subjects with COPD[54-56]. The identification of COPD phenotypes appears as one of the current major challenges in subjects with COPD. Many statistical methods have been proposed to examine phenotypic heterogeneity of COPD[55, 56]. Clustering analysis is a statistical method which transforms heterogeneous groups of variables into relatively homogenous groups with the use of advanced machine learning capabilities. In the future, we will use this cluster analysis on the larger dataset to test the hypothesis that the lung biomechanical features with other CT derived features could lead to grouping of COPD subjects according to phenotypic characteristics.

CHAPTER 6

CONCLUSION

This study demonstrates the effectiveness of the registration based estimates of lung tissue expansion and contraction in recognizing COPD and its severity. Three measures were extracted from the registered scans and the features based on these three measures showed good correlations with the pulmonary function. All the experiments illustrated that the classification is improved at both COPD/Non-COPD and severity stage classification with the inclusion of proposed lung biomechanical features to the existing density and texture based features. With further testing on larger databases, the proposed approach may be used for accurate measure of the pulmonary function and disease.

APPENDIX

The demographic information of all the subjects used in this study collected from COPDGene database.

COPDGENE UIA #ID	AGE	GENDER	BMI	FEV$_1$/FVC	FEV$_1$% PRED	GOLD STAGE
18666W	61	F	25	0.88	1.16	Normal
18747W	60	F	26	0.78	0.92	Normal
18749A	76	F	41.7	0.82	0.85	Normal
18757Z	71	F	28.5	0.77	1.01	Normal
18765Y	70	M	25.8	0.87	1.20	Normal
18825Q	76	F	29.1	0.87	1.39	Normal
19020F	58	F	24.3	0.72	1.00	Normal
18826S	74	M	25.3	0.86	1.13	Normal
18763U	72	M	26.4	0.81	1.25	Normal
18734N	74	F	30.5	0.8	0.82	Normal
18782Y	65	M	28.1	0.84	0.91	Normal
18810D	79	F	35.2	0.84	0.96	Normal

Table A1: Demographic and spirometry information per subject (Continued)

COPDGENE UIA #ID	AGE	GENDER	BMI	FEV$_1$/FVC	FEV$_1$% PRED	GOLD STAGE
18977N	71	M	28.7	0.74	0.87	Normal
10233D	61	M	27.4	0.72	0.95	GOLD0
10223A	67	M	32	0.79	0.89	GOLD0
10263M	61	F	27.7	0.76	1.00	GOLD0
10252H	63	F	31.2	0.79	1.07	GOLD0
10396F	67	M	23	0.72	0.90	GOLD0
10265Q	66	F	27.2	0.78	0.90	GOLD0
10443O	55	M	34.8	0.84	0.90	GOLD0
10101M	61	F	24.2	0.74	0.93	GOLD0
10123W	58	M	26.8	0.8	0.92	GOLD0
10124Y	65	M	31.8	0.8	0.9	GOLD0
10127E	61	F	22.6	0.83	0.91	GOLD0
10151B	76	M	25	0.76	0.92	GOLD0
10153F	66	M	29.4	0.74	0.91	GOLD0
10155J	64	F	27	0.7	0.95	GOLD0
10189A	80	M	29.3	0.71	0.96	GOLD0
10305C	76	M	23.7	0.56	0.93	GOLD1

Table A1 continued

COPDGENE UIA #ID	AGE	GENDER	BMI	FEV$_1$/FVC	FEV$_1$% PRED	GOLD STAGE
10736D	78	F	39.9	0.56	0.81	GOLD1
10921Y	63	M	24.9	0.6	0.88	GOLD1
11506R	69	F	23.1	0.55	0.91	GOLD1
11113Y	70	F	22	0.65	1.05	GOLD1
11558K	68	F	22.9	0.58	0.80	GOLD1
11570A	77	F	22.5	0.66	1.04	GOLD1
10312Z	68	F	21.9	0.64	0.98	GOLD1
10313B	71	M	30.1	0.63	0.90	GOLD1
10569K	69	M	27.8	0.66	1.12	GOLD1
10598R	64	M	23.7	0.65	0.82	GOLD1
10603K	65	F	22.1	0.59	0.91	GOLD1
10307G	67	F	20.2	0.53	0.81	GOLD1
10190L	78	F	29.1	0.47	0.86	GOLD1
10253J	73	M	28.1	0.66	0.94	GOLD1
10192P	63	F	32.5	0.69	0.65	GOLD2
10457Z	68	F	26.3	0.68	0.74	GOLD2
10601G	65	M	40.5	0.66	0.71	GOLD2

Table A1 continued

COPDGENE UIA #ID	AGE	GENDER	BMI	FEV$_1$/FVC	FEV$_1$% PRED	GOLD STAGE
10624S	70	M	31.8	0.48	0.61	GOLD2
10691H	69	M	23.3	0.63	0.78	GOLD2
10641S	76	M	24.1	0.57	0.65	GOLD2
10704Q	69	F	22.7	0.65	0.61	GOLD2
10125A	63	M	33.3	0.63	0.65	GOLD2
10126C	72	F	26.9	0.53	0.74	GOLD2
10130T	64	F	32.4	0.57	0.77	GOLD2
10141Y	65	F	28.7	0.51	0.56	GOLD2
10160C	68	M	20.6	0.55	0.54	GOLD2
10164K	65	F	40.8	0.66	0.62	GOLD2
10179X	70	F	32.5	0.59	0.59	GOLD2
10205Y	62	F	25.7	0.6	0.69	GOLD2
11875W	70	M	25.4	0.36	0.33	GOLD3
12001S	62	M	31	0.33	0.41	GOLD3
12250N	68	F	19	0.35	0.30	GOLD3
12608E	64	M	27.4	0.39	0.35	GOLD3
13042L	76	M	30.3	0.32	0.45	GOLD3

Table A1 continued

COPDGENE UIA #ID	AGE	GENDER	BMI	FEV$_1$/FVC	FEV$_1$% PRED	GOLD STAGE
13059C	56	F	42.8	0.64	0.43	GOLD3
13145V	73	M	33	0.45	0.49	GOLD3
10719D	72	M	30.3	0.41	0.42	GOLD3
11201V	72	M	27.8	0.31	0.39	GOLD3
11703T	76	M	31.6	0.39	0.39	GOLD3
11750C	71	F	25.8	0.52	0.40	GOLD3
11754K	64	F	34.8	0.26	0.31	GOLD3
10503G	75	M	27.2	0.33	0.33	GOLD3
10708Y	69	M	28.1	0.4	0.44	GOLD3
10571X	68	F	27	0.36	0.40	GOLD3
14192J	63	F	20.1	0.17	0.12	GOLD4
16104W	64	M	21.3	0.26	0.10	GOLD4
15690E	64	F	25.9	0.3	0.28	GOLD4
15284T	45	F	20.6	0.28	0.22	GOLD4
17173U	61	M	33.5	0.33	0.24	GOLD4
16294B	68	M	46.1	0.39	0.24	GOLD4
21700T	62	M	25.5	0.22	0.24	GOLD4

Table A1 continued

COPDGENE UIA #ID	AGE	GENDER	BMI	FEV$_1$/FVC	FEV$_1$% PRED	GOLD STAGE
13344B	69	F	25.7	0.35	0.22	GOLD4
13383L	63	F	25.7	0.31	0.22	GOLD4
14197T	70	M	39.2	0.24	0.28	GOLD4
14538T	71	M	27.4	0.25	0.23	GOLD4
14880F	67	M	33.7	0.24	0.28	GOLD4
24383W	67	F	15.4	0.35	0.29	GOLD4
15861F	55	F	26	0.32	0.26	GOLD4
15811Q	71	M	28.4	0.23	0.23	GOLD4

Table A1 continued

REFERENCES

1. Rabe KF, Hurd S, Anzueto A, Barnes PJ, Buist SA, Calverley P, Fukuchi Y, Jenkins C, Rodriguez-Roisin R, van Weel C, Zielinski J, Global Initiative for Chronic Obstructive Lung D. Global strategy for the diagnosis, management, and prevention of chronic obstructive pulmonary disease: Gold executive summary. *American journal of respiratory and critical care medicine*. 2007;176:532-555

2. GOLDCOPD. From the global strategy for the diagnosis, management and prevention of copd, global initiative for chronic obstructive lung disease (gold) 2011. . 2011

3. Gurney JW, Jones KK, Robbins RA, Gossman GL, Nelson KJ, Daughton D, Spurzem JR, Rennard SI. Regional distribution of emphysema: Correlation of high-resolution ct with pulmonary function tests in unselected smokers. *Radiology*. 1992;183:457-463

4. Dirksen A, Holstein-Rathlou NH, Madsen F, Skovgaard LT, Ulrik CS, Heckscher T, Kok-Jensen A. Long-range correlations of serial fev1 measurements in emphysematous patients and normal subjects. *Journal of applied physiology*. 1998;85:259-265

5. Bafadhel M, Umar I, Gupta S, Raj JV, Vara DD, Entwisle JJ, Pavord ID, Brightling CE, Siddiqui S. The role of ct scanning in multidimensional phenotyping of copd. *Chest*. 2011;140:634-642

6. Lynch DA, Newell JD. Quantitative imaging of copd. *Journal of thoracic imaging*. 2009;24:189-194

7. Gevenois PA, de Maertelaer V, De Vuyst P, Zanen J, Yernault JC. Comparison of computed density and macroscopic morphometry in pulmonary emphysema. *American journal of respiratory and critical care medicine*. 1995;152:653-657

8. Muller NL, Staples CA, Miller RR, Abboud RT. "Density mask". An objective method to quantitate emphysema using computed tomography. *Chest*. 1988;94:782-787

9. Muller NL, Thurlbeck WM. Thin-section ct, emphysema, air trapping, and airway obstruction. *Radiology*. 1996;199:621-622

10. Busacker A, Newell JD, Jr., Keefe T, Hoffman EA, Granroth JC, Castro M, Fain S, Wenzel S. A multivariate analysis of risk factors for the air-trapping asthmatic phenotype as measured by quantitative ct analysis. *Chest*. 2009;135:48-56

11. Newman KB, Lynch DA, Newman LS, Ellegood D, Newell JD, Jr. Quantitative computed tomography detects air trapping due to asthma. *Chest*. 1994;106:105-109

12. Hoffman EA, Reinhardt JM, Sonka M, Simon BA, Guo J, Saba O, Chon D, Samrah S, Shikata H, Tschirren J, Palagyi K, Beck KC, McLennan G. Characterization of the interstitial lung diseases via density-based and texture-based analysis of computed tomography images of lung structure and function. *Academic radiology*. 2003;10:1104-1118

13. Sorensen L, Nielsen M, Lo P, Ashraf H, Pedersen JH, de Bruijne M. Texture-based analysis of copd: A data-driven approach. *IEEE transactions on medical imaging*. 2012;31:70-78

14. Sorensen L, Shaker SB, de Bruijne M. Quantitative analysis of pulmonary emphysema using local binary patterns. *IEEE transactions on medical imaging*. 2010;29:559-569

15. Uppaluri R, Mitsa T, Sonka M, Hoffman EA, McLennan G. Quantification of pulmonary emphysema from lung computed tomography images. *American journal of respiratory and critical care medicine*. 1997;156:248-254

16. Xu Y, Sonka M, McLennan G, Guo J, Hoffman EA. Mdct-based 3-d texture classification of emphysema and early smoking related lung pathologies. *IEEE transactions on medical imaging*. 2006;25:464-475

17. Ding K, Yin Y, Cao K, Christensen GE, Lin CL, Hoffman EA, Reinhardt JM. Evaluation of lobar biomechanics during respiration using image registration. *Medical image computing and computer-assisted intervention : MICCAI ... International Conference on Medical Image Computing and Computer-Assisted Intervention*. 2009;12:739-746

18. Murphy K, Pluim JP, van Rikxoort EM, de Jong PA, de Hoop B, Gietema HA, Mets O, de Bruijne M, Lo P, Prokop M, Ginneken B. Toward automatic regional analysis of pulmonary function using inspiration and expiration thoracic ct. *Medical physics*. 2012;39:1650-1662

19. Reinhardt JM, Ding K, Cao K, Christensen GE, Hoffman EA, Bodas SV. Registration-based estimates of local lung tissue expansion compared to xenon ct measures of specific ventilation. *Medical image analysis*. 2008;12:752-763

20. Van Rikxoort EM DJP, Mets OM and Van Ginneken B. Automatic classification of pulmonary function in copd patients using trachea analysis in chest ct scans. . *SPIE*. 2012

21. Gould GA, MacNee W, McLean A, Warren PM, Redpath A, Best JJ, Lamb D, Flenley DC. Ct measurements of lung density in life can quantitate distal airspace enlargement--an essential defining feature of human emphysema. *The American review of respiratory disease*. 1988;137:380-392

22. Gould GA, Redpath AT, Ryan M, Warren PM, Best JJ, Flenley DC, MacNee W. Lung ct density correlates with measurements of airflow limitation and the diffusing capacity. *The European respiratory journal : official journal of the European Society for Clinical Respiratory Physiology*. 1991;4:141-146

23.   Newell JD, Jr., Hogg JC, Snider GL. Report of a workshop: Quantitative computed tomography scanning in longitudinal studies of emphysema. *The European respiratory journal : official journal of the European Society for Clinical Respiratory Physiology*. 2004;23:769-775

24.   Shaker SB, Dirksen A, Laursen LC, Maltbaek N, Christensen L, Sander U, Seersholm N, Skovgaard LT, Nielsen L, Kok-Jensen A. Short-term reproducibility of computed tomography-based lung density measurements in alpha-1 antitrypsin deficiency and smokers with emphysema. *Acta radiologica*. 2004;45:424-430

25.   Matsuoka S, Kurihara Y, Yagihashi K, Hoshino M, Watanabe N, Nakajima Y. Quantitative assessment of air trapping in chronic obstructive pulmonary disease using inspiratory and expiratory volumetric mdct. *AJR. American journal of roentgenology*. 2008;190:762-769

26.   Lee TA, Bartle B, Weiss KB. Spirometry use in clinical practice following diagnosis of copd. *Chest*. 2006;129:1509-1515

27.   Murphy k, van Ginneken B, Van Rikxoort EM, de Hoop BJ, Prokop M, Lo P, de Bruijne M and Pluim JPW. . Obstructive pulmonary function: Patient classification using 3d registration of inspiration and expiration ct images.

28.   Lederman D LJ, Zheng B, Sciurba FB, Tan J and Gur D. Quantitative computed tomography of lung parenchyma in patients with emphysema: Analysis of higher density lung regions. *SPIE*. 2011

29.   Park YS, Seo JB, Kim N, Chae EJ, Oh YM, Lee SD, Lee Y, Kang SH. Texture-based quantification of pulmonary emphysema on high-resolution computed tomography: Comparison with density-based quantification and correlation with pulmonary function test. *Investigative radiology*. 2008;43:395-402

30.   Sakai N, Mishima M, Nishimura K, Itoh H, Kuno K. An automated method to assess the distribution of low attenuation areas on chest ct scans in chronic pulmonary emphysema patients. *Chest*. 1994;106:1319-1325

31.   Amelon R, Cao K, Ding K, Christensen GE, Reinhardt JM, Raghavan ML. Three-dimensional characterization of regional lung deformation. *Journal of biomechanics*. 2011;44:2489-2495

32.   National Institute of Health. NIH. COPD. 2010

33.   Xu Y, van Beek EJ, Hwanjo Y, Guo J, McLennan G, Hoffman EA. Computer-aided classification of interstitial lung diseases via mdct: 3d adaptive multiple feature method (3d amfm). *Academic radiology*. 2006;13:969-978

34.   Xu YS, M. McLennan, G. Guo J and Hoffman EA. Sensitivity and specificity of 3d texture analysis of lung parenchyma is better than 2d for discrimination of lung pathology in stage 0 copd. *SPIE*. 2005

35.   Hoffman EA, McLennan G. Assessment of the pulmonary structure-function relationship and clinical outcomes measures: Quantitative volumetric ct of the lung. *Academic radiology*. 1997;4:758-776

36.   Analyze Image Processing Software. Mayo Clinic. Rochester. NY.

37.   Galvin I, Drummond GB, Nirmalan M. Distribution of blood flow and ventilation in the lung: Gravity is not the only factor. *British journal of anaesthesia*. 2007;98:420-428

38.   Gee J, Sundaram T, Hasegawa I, Uematsu H, Hatabu H. Characterization of regional pulmonary mechanics from serial magnetic resonance imaging data. *Academic radiology*. 2003;10:1147-1152

39.   Luis Ib´a˜nez WS, Lydia Ng, Josh Cates, and the Insight Software Consortium. The itk software guide, second edition, updated for itk version 2.4. 2005

40.   Cao K, Christensen, G.E., Ding, K., Reinhardt, J.M. Intensity-and-landmark-driven, inverse consistent, b-spline registration and analysis forlung imagery. *Second International Workshop on Pulmonary Image Analysis*. 2009

41.   Yin Y, Hoffman EA, Lin CL. Mass preserving nonrigid registration of ct lung images using cubic b-spline. *Medical physics*. 2009;36:4213-4222

42.   Cao K. Local lung tissue expansion analysis based on inverse consistent image registration. *Electrical and Computer Engineering*. 2008

43.   Foreman MG, DeMeo DL, Hersh CP, Reilly JJ, Silverman EK. Clinical determinants of exacerbations in severe, early-onset copd. *The European respiratory journal : official journal of the European Society for Clinical Respiratory Physiology*. 2007;30:1124-1130

44.   Christensen GE, Rabbitt, R.D., Miller, M.I., Joshi, S., Grenander, U., Coogan, T., Essen, D.V. Topological properties of smooth anatomic maps. *Information Proceedings in Medical Imaging*. 1995;3

45.   RC B. *Advanced calculus*. St. Louis: McGraw-Hill Book Company; 1978.

46.   Lubliner J. *Plasiticity theory*. Mineola, NY: Dover Publication; 2008.

47.   Pellegrino R, Viegi G, Brusasco V, Crapo RO, Burgos F, Casaburi R, Coates A, van der Grinten CP, Gustafsson P, Hankinson J, Jensen R, Johnson DC, MacIntyre N, McKay R, Miller MR, Navajas D, Pedersen OF, Wanger J. Interpretative strategies for lung function tests. *The European respiratory journal : official journal of the European Society for Clinical Respiratory Physiology*. 2005;26:948-968

48.   Gutlein M FE, Hall M, and Karwath A. Large-scale attribute selection using wrappers. . 2009

49.   Mark Hall EF, Geoffrey Holmes, Bernhard Pfahringer, Peter Reutemann, Ian H. Witten. The weka data mining software: An update; sigkdd explorations,. 2009

50.   Aha D.W. KD, and Albert M.K. Instance-based learning algorithms. *Machine Learning*. 1991

51.   Sluimer IC, van Waes PF, Viergever MA, van Ginneken B. Computer-aided diagnosis in high resolution ct of the lungs. *Medical physics*. 2003;30:3081-3090

52. Yavarna T. Airway segmentation of the ex-vivo mouse lung volume using voxel based classification. *Biomedical Engineering*. 2011;Masters of Science

53. Newell JD, Jr. Quantitative computed tomography of lung parenchyma in chronic obstructive pulmonary disease: An overview. *Proceedings of the American Thoracic Society*. 2008;5:915-918

54. Bourdin A, Burgel PR, Chanez P, Garcia G, Perez T, Roche N. Recent advances in copd: Pathophysiology, respiratory physiology and clinical aspects, including comorbidities. *European respiratory review : an official journal of the European Respiratory Society*. 2009;18:198-212

55. Burgel PR, Paillasseur JL, Caillaud D, Tillie-Leblond I, Chanez P, Escamilla R, Court-Fortune I, Perez T, Carre P, Roche N, Initiatives BSC. Clinical copd phenotypes: A novel approach using principal component and cluster analyses. *The European respiratory journal : official journal of the European Society for Clinical Respiratory Physiology*. 2010;36:531-539

56. Weatherall M, Travers J, Shirtcliffe PM, Marsh SE, Williams MV, Nowitz MR, Aldington S, Beasley R. Distinct clinical phenotypes of airways disease defined by cluster analysis. *The European respiratory journal : official journal of the European Society for Clinical Respiratory Physiology*. 2009;34:812-818